IEEE Journal of Microwaves

Received 6 April 2023; revised 29 May 2023 and 10 June 2023; accepted 11 June 2023. Date of publication 10 July 2023; date of current version 9 October 2023.

Digital Object Identifier 10.1109/JMW.2023.3285825

A Comprehensive Survey on Transmitting Antenna Systems With Synthesized Beams for Microwave Wireless Power Transmission

PING LU [1] (Member, IEEE), MAHMOUD WAGIH [2] (Member, IEEE), GEORGE GOUSSETIS [3] (Senior Member, IEEE), NAOKI SHINOHARA [4] (Senior Member, IEEE), AND CHAOYUN SONG [5] (Senior Member, IEEE)

(Invited Paper)

[1]School of Electronics and Information Engineering, Sichuan University, Chengdu, Sichuan 610065, China
[2]James Watt School of Engineering, University of Glasgow, G12 8QQ Glasgow, U.K.
[3]School of Engineering and Physical Science, Heriot-Watt University, EH14 4AS Edinburgh, U.K.
[4]Research Institute for Sustainable Humanosphere, Kyoto University, Uji, Kyoto 611-0011, Japan
[5]Department of Engineering, King's College London, WC2R 2LS London, U.K.

CORRESPONDING AUTHORS: Ping Lu; Chaoyun Song (e-mail: pinglu90@scu.edu.cn; chaoyun.song@kcl.ac.uk).

This work was supported in part by the National Key R&D Program of China under Grant 2021YFB3900300, in part by the National Key Laboratory Foundation under Grants 2021-JCJQ-LB-006 6142411212106, in part by the EPSRC (U.K.), in part by the U.K. Royal Academy of Engineering and the Office of the Chief Science Adviser for National Security through the U.K. Intelligence Community Research Fellowship Programme, and in part by the National Natural Science Foundation of China under Grant 51907130.

ABSTRACT In recent years, microwave wireless power transmission (MWPT) has emerged as a promising technology for supplying energy by receiving radiative power without wires and converting it into DC power. A high transmission efficiency is crucial for improving the performance of MWPT systems. To address the challenge of propagation loss, beam synthesis using transmitting antennas has gained significant attention, resulting in several synthesis methods becoming available, including whisper beams, flat-top beams, non-diffractive beams, supergain/superdirective beams, focused beams and adaptive beamforming technique such as time reversal methods. This comprehensive review covers these advanced beam synthesis techniques for MWPT transmitters and provides a detailed comparison of different synthesized beams. The article includes an in-depth discussion on current designs and existing technological challenges, as well as suggestions for future research directions. Although beam synthesis can substantially improve the transmission efficiency, the overall power transfer efficiency of the entire MWPT system still requires improvement as the performance, including impedance matching, is currently only considered at a component level and not at a system level. Furthermore, when using advanced beam synthesis techniques, the engineering and implementation challenges of high power ($\geq$kW) and long-distance ($\geq$km) MWPT become significant issues due to the high cost and large size involved. The review concludes that existing technologies for synthesized beams still require significant long-term efforts to meet the realistic engineering requirements for achieving highly efficient MWPT systems. The joint utilization of beam synthesis techniques and comprehensive system matching/optimization is identified as a research direction with the potential to realize highly efficient MWPT systems, offering foreseeable impacts in both terrestrial and space-based MWPT applications. This review serves as a solid foundation for the design of transmitter antennas in long-distance, high-power MWPT systems, and furthermore provides novel insights for future designs of highly efficient MWPT systems.

INDEX TERMS Beam synthesis technology, rectennas, wireless power transfer, flattop beam, non-diffractive beam, supergain/superdirective beam, focused beam, time reversal, adaptive beamforming technique.

I. INTRODUCTION

Microwave Wireless Power Transmission (MWPT), where physical wire and connections are not required, delivers the radio frequency (RF) power via microwaves in free space, and then converts RF power into direct current (DC) power, as displayed in Fig. 1 [1], [2]. For example, the solar power is transmitted from space to earth land [3], and then being converted to electricity. The offshore wind farms deliver electricity to areas with difficult natural conditions such as remote mountains. Due to long distance for transmission, MWPT has advantages over other wireless power transmission technologies, e.g., electromagnetic coupling and magnetic resonance. Recently, using such a technology has promoted the development of microsystem power supply, wireless charging and green radio communications.

The comprehensive research concerning long-distance high-power MWPT system at the earliest stage appeared in the United States. In 1899, the first microwave wireless energy transmission experiment was completed by Tesla [4], [5], [6]. In 1957, the Jet Propulsion Laboratory (JPL) carried out an important MWPT experiment, which was the world's first long-distance MWPT experiment. The experiment was carried out in the Mohave Desert in a transmission distance of 1.6 km at operation frequency of 2.388 GHz. The experiment successfully received 30 kW DC power when transmitting microwave power was 450 kW [7]. In 1964, W. Brown built a platform to drive the levitation device by wireless microwave energy, and the device successfully flew for 10 hours at an altitude of 50 ft [8]. As time goes by, MWPT has attracted a strong interest from researchers in Japan and Europe. In 1992, the microwave was transmitted from the car into the aircraft, and the aircraft position was tracked by beam scanning. The system operated at 2.4 GHz, and the RF-dc conversion efficiency achieved 54% [9]. Then, the ground MWPT experiment was carried out. In 2001, a point-to-point MWPT system was set up in Reunion Island, which successfully transmitted 10 kW of the electricity to villages at the bottom of the valley [10]. In 2008, the RF power was transmitted from Maui to Hawaii over a distance of 148 km, which created a new distance record. In 2015, the Japanese aerospace exploration agency (JAXA) had carried out a ground MWPT test in a transmission distance of 55 m. The system operated at 5.8 GHz for the 1.8 kW transmitting power, and the efficiency was 18.89%. In the same year, another ground MWPT experiment was implemented. The system delivered RF power of 10 kW and received electromagnetic energy through a rectenna array, which was 500 m away from the transmitters [11]. Recently, a rapid demonstration at X band in Blossom Point delivered 1.6 kW of electrical power at a 1046 m standoff. Considering the effects of microwave propagation across terrain, the efficiency achieved 1.8% [12]. These experiments reveal MWPT at high transmitting power (≥kW) in long distance (≥km) is successfully implemented, but the efficiency is not high [13].

To investigate the reasoning of low WPT efficiency, the MWPT experiment showed that 42% of RF power is reflected at the receiving antenna with only 39% power delivery to rectifiers, and accordingly the transmission-conversion efficiency is only 14.8% for overall system efficiency, as displayed in Fig. 1 [14]. To improve the system efficiency, the beam transmission between transmitters and receivers was investigated [15]. It is found that the special aperture field distributions on the transmitters and receivers are required for maximum efficiency. A major effort is under way to achieve the special aperture field distributions. Therefore, an in-depth and critical review on synthesized beam for wireless power transmitters is essentially useful. The review should not just discuss the existing technologies, but more important about the upcoming and emerging challenges.

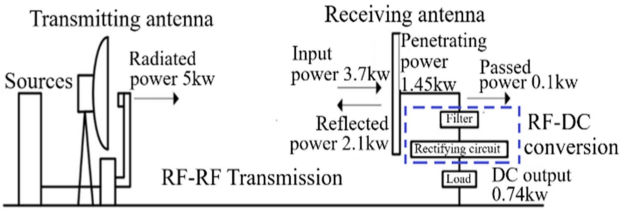

FIGURE 1. Energy distribution in each part of MWPT system [10]. The MWPT system consists of three parts. (1) DC-RF conversion: The transmitting antenna, connected with a microwave power source, is responsible for converting DC power into RF power. This RF power is then efficiently radiated into free space. (2) RF-RF transmission: The RF power propagates through the free space, and the beam is received by the receiving antenna. (3) RF-DC conversion: The receiving antenna captures the RF power present in free space, which is subsequently input to the rectifying circuit. The rectifying circuit converts the RF power into DC power.

This article aims to conduct a thorough and comprehensive review of the advanced technology of synthesized beams in the field of MWPT. It highlights past development efforts, reviews state-of-the-art technologies, and explores available ways forward for the future. The remaining sections of this article are organized as follows: Section II presents the MWPT system and introduces the features of each part. Section III reviews the advanced technology for beam transmission between transmitters and receivers, summarizing the advantages and disadvantages of each method. Additionally, advanced antenna designs with special aperture field distributions are introduced. Section IV provides a critical discussion of the advanced techniques presented in Section III. Finally, the future research directions and technical recommendations are summarized and presented in the concluding section.

II. MWPT SYSTEM

Coupled systems are restricted to the near-field, as their efficiency is restricted by a $1/r^6$ coupling between the transmitting and receiving magnetic dipoles [16]. Moving to the radiative "Fresnel" near-field and far-field region, the microwave radiation is required to transfer high power levels over long-range distances instead of using the coupling strategy. The increased research interest across all MWPT technologies is reflected in the volume of recent literature

TABLE 1. Related Reviews on Radiative Wireless Power

MWPT area	Review Papers
Rectifier design	Modelling and energy harvesting [17]
Power beaming	Historical trends and overview [13], [19]
Application-specific	Wearables [20], [21], Additive and flexible devices [22]. Metasurfaces and arrays [23], [24], [25], [26]
Beam synthesis (This review)	**Advanced synthetic beams**

concerned with MWPT. Table 1 shows a summary of the recent reviews dealing with MWPT, and highlights the key focus of this article, i.e., the synthesis of advanced beams for MWPT.

As displayed in Fig. 1, the MWPT system is composed of four parts: microwave sources, transmitting antenna, receiving rectenna (i.e., antenna plus rectifying circuit) and dc load. The microwave sources (e.g., signal sources and magnetrons) will convert the electricity into microwaves where the transmitting antennas can effectively radiate the microwave signal in the form of electromagnetic waves in free space. As a receiver, the rectenna consists of receiving antenna and rectifying circuit, in which the antenna receives RF power on the aperture, and then converts it into dc power by using rectifying circuit [26]. The process from transmitting antenna to the DC load mainly includes the microwave power transmission and RF-DC power conversion. Thus, the MWPT system efficiency, the RF-RF transmission efficiency η_{tr} (including the aperture efficiency and radiation efficiency) and RF-DC conversion efficiency η_{dc}, are the important parameters for the quantitative evaluation of system performance [28].

To improve the system efficiency, some automatically tuning antennas were designed for good impedance matching to optimize MWPT system [29], [30]. On the other hand, some advanced technologies for synthesizing beams were proposed for improving the transmission and/or conversion efficiency. In beam synthesis, the aperture field distribution is optimized in the transmitting antenna to increase the beam power, ultimately enabling more RF power to be delivered to the receiver. In addition, the transmitted beam is synthesized to achieve uniform aperture field distribution for maintaining a high conversion efficiency, at the receiver, for varying angles of incidence and application scenarios. In the next section, we study the advanced antennas and beam synthesis techniques to identify their special characteristics, pros and cons.

III. ADVANCED BEAM SYNTHESIS TECHNIQUES

To achieve high transmission efficiency, the beam synthesis techniques are the fundamental necessity for good transmitting antennas design: different special field distributions may result in diverse designs and performances. For MWPT system, effective point-to-point beam forming with high transmission efficiency requires the appropriately shaped beam to extract the optimal performance of receivers (rectennas).

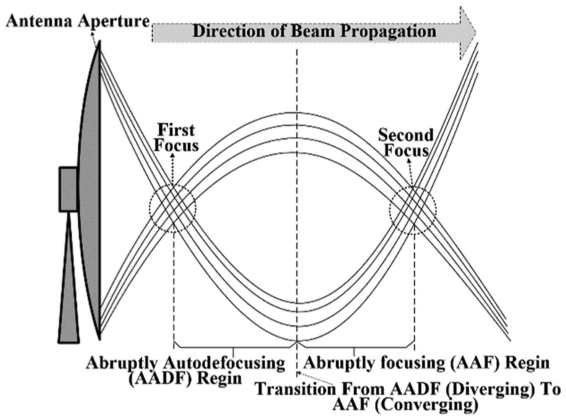

FIGURE 2. Whisper beams [32].

Gaussian beam is a typical technique for spatial power combining [29], which will not be further discussed in this article. The main beam patterns of interest to us are the whisper beam, the flat-top beam, the non-diffractive beam, the supergain beam, focused beam and the adaptive beamforming technique, including the time- reversal.

A. WHISPER BEAM (AIRY BEAMS)

Whisper beams can focus high power for long-distance wireless power transmission. Whisper beams are generally categorized as non-Gaussian beam, i.e., they are formed by two Airy beams [32], [33], which are twisted in the opposite direction. Note that here the whisper beam is different from the Whispering Gallery mode of dielectric antennas. For Whisper beams, the beam with mirror-symmetric autofocusing is formed at a first focus at wavelengths, and is then dispersed in an abruptly auto-defocusing patterns (AADF), which passes through the focal point and spreads itself out to a large circular Airy beam with a diffuse core. Subsequently, the diffused beams in Airy profile are abruptly autofocusing (AAF region) in a second focus, which is formed in the transitions from AADF to AAF. This is displayed in Fig. 2, where a parabolic path for the electromagnetic waves is generated [34]. It is noticed that the electromagnetic energy is dispersed between the transmitter and the receiver, and then recombined at the receiver.

When implementing whisper beams, the transmitting antenna and the receiver are located at or nearby the first and second focus point, respectively. In the transition from diverging to converging, the field strength between the two focal regions (called the auto-defocusing zone) become very low. Therefore, foreign objects such as humans, vehicles, or other equipment in this region will not be exposed to high electromagnetic field strength due to being in the auto-defocusing area. Due to the self-healing property of the whisper beam, the electromagnetic energy can be captured at the receiver with the transmission path being partially obstructed by objects like walls. The benefit of this advanced technology is that power remains diffuse in most of the area between the transmitters and receivers. Even if the receiver in the second focus area

receives megawatts of power, far less power is concentrated in the region ahead the focus area. The beam would have little impacts on unintended humans, wildlife, aircraft, and vehicles that may inadvertently wander into the beam. Hence, Whisper beams are widely used for wireless power transmission in high power level with human activities to protect the safety [34].

For high power level and long transmission range at microwaves, a two-dimensional axisymmetric array with millions of antenna elements is employed. By using paraxial diffraction equations, the phase and amplitude of each element excitation should be precisely controlled for the whisper beam generation. To produce a larger aperture, it is expected to increase the number of transmitter elements. To address this challenge, the antenna elements can be arranged at an irregular spacing, and the sparse array, which achieves an effectively wider aperture with much less element number, is created rather than the axisymmetric array.

The next challenge is to expand the operation frequency of optics to microwaves. Although the whisper beam array can be, theoretically, applied in microwave bands, engineering difficulties are encountered in the implementation due to very large aperture required. Besides, the two foci are only 20 wavelengths apart [34], indicating that the transmitter and receiver are placed within 20 wavelengths, and the propagation distance is limited.

B. FLAT-TOP BEAM

Due to the nonlinearity of rectifier diode, the RF-DC conversion efficiency varies as a function of the input power. On the aperture of the receiving antenna, the power density changes as a function of the angle off the antenna's main lobe. Therefore, the rectifier's efficiency deteriorates beyond the optimum operation power ranges of the rectifier P_{diode}. For high conversion efficiency, the receiving antenna should be reasonably deployed to achieve the P_{diode}. According to power levels in different zones, a non-uniform receiving antenna array consisting of the antenna subarrays with different sizes was proposed [35]. However, additional complicated feeding network is required for the receiving antenna array.

To improve the resilience to angular misalignment, the flat-top beam with uniform power density is of great significance for the receiver. The concept of flat-top beam was initially proposed in wireless communication area to expand the wireless access range with the homogeneous availability [36]. This technology is suitable for beam forming to produce uniform illumination on the receiving aperture. It is demonstrated that the conversion efficiency of the rectifying circuit array was greatly improved due to the uniform illumination with flat-top beam [37]. To radiate the flat-top beam, the specific excitation of amplitude and phase is required for transmitting elements. Since the amplitude excitation is analogous to sync-function with uneven power for each antenna [38], the transmitting antenna designs with desired amplitude and phase excitation for flat-top beam are extremely challenging.

To achieve a flat-top beam pattern, a compact double-shell lens antenna was designed in the 28-GHz band. The lens shape

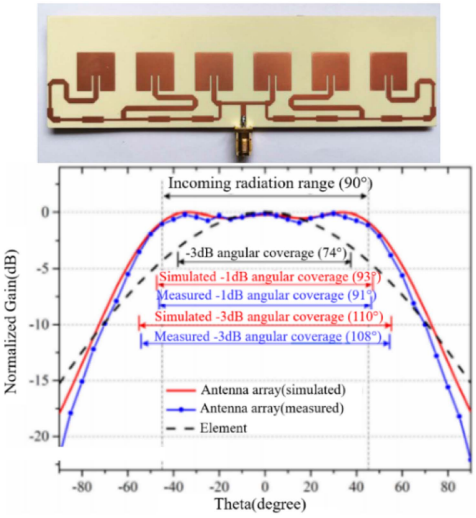

FIGURE 3. Six-element microstrip patch antenna array with flattop beam pattern [43].

was optimized, and the primary feed pattern is converted to an axis-symmetrical flat-top beam [37]. Typical methods for various antennas/antenna arrays can be found in the literature by optimizing the desired amplitude and phase excitation [40]. One example was given in [41]. By using genetic algorithm, a ten-element antenna array was presented with optimized amplitude and phase excitations for a flat-top pattern in the main beam, where a well-proportioned power distribution is achieved. In different application scenarios, a wideband antenna is proposed for the desired operational frequency. In [42], a wideband antenna array with 10-element bowtie dipole antennas is presented. By using self-adaptive differential evolution algorithm, the feed network with desired amplitude and phase distribution are designed for flat top beam generation.

Beam steering is an attractive way for tracking single to multi-point and moving target systems. For the flat-top beam steering, the designed antennas are required to provide stable and wide-angle scanning with similar gain in all directions by modifying the amplitude and phase along the feed of the array element with low complexity. For maximum power transmission efficiency, a six-element receiving array was proposed to achieve a flat top wide beam, based on the quadratically constrained quadratic programing, as displayed in Fig. 3 [43]. However, the proposed flat-top antenna required a complex feeding mechanism. In [44], by using Graded Index Metasurface Lens (GIML), a low-profile lens antenna features a flat-top beam whose angular coverage is adjustable, as shown in Fig. 4. The metasurface lens is composed of an ultrathin linear GIML and the radial GIML was placed on the top of the microstrip antenna. Due to the magnitude and phase transformation on the metasurface lens, the radiated beam from the antenna can be manipulated for flat-top beam steering. Besides, by using leaky wave mode, a substrate integrated waveguide antenna is presented for flat-top beam-steering with double-layered vertically stacked structure. To obtain

TABLE 2. Summary of Preceding Flat-Top Antenna Designs

Ref.	Freq. (GHz)	Feeding network	Element number	HPBW (deg)	Sidelobes (dB)	Efficiency (%)	Design complexity	Applications
[37]	28	Double shell	1	Over 80	-15	-	Moderate	Single target or fixed target
[41]	1.71-1.74	Microstrip power divider	10	Over 40	-20	-	Simple	Single target or fixed target
[42]	1.1-1.6	Microstrip (Parallel and series feed)	10	30	-13.7	-	Moderate	Single target or fixed target
[43]	5.8	Microstrip (Series feed)	6	108	-	60.1	Simple	Multi-target or moving target
[44]	10.1	Metasurface	76	Over 34	-10	-	Moderate	Multi-target or moving target
[45]	15	SIW leaky-wave	16	30	-10	75	Moderate	Multi-target or moving target
[46]	5.74	Microstrip (Series feed)	196	10	-	32	Complex	Single target or fixed target

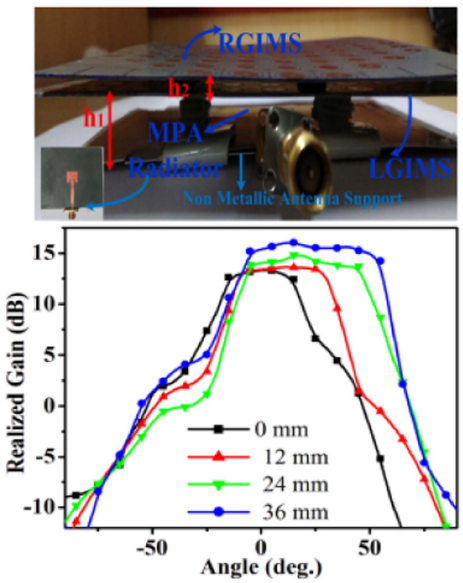

FIGURE 4. Gain patterns of a lens antenna with a flat-top beam [44].

desired flat-top pattern in all the scanning directions, the leaky wave mode parameters e.g., the attenuation and phase constants, are controlled independently [45]. However, the feeding network is overly complicated for a large-scale phased array.

Should a compact antenna aperture with a small number of array elements be used? A main beam with a large half-power beamwidth (HPBW) is expected, leading to a poor point-to-point transmission efficiency due to low gain. To obtain the narrow beam, a large-scale sequential phased array at C-band was designed to implement flat beams by using Woodward Lawson method, as displayed in Fig. 5 [46]. For

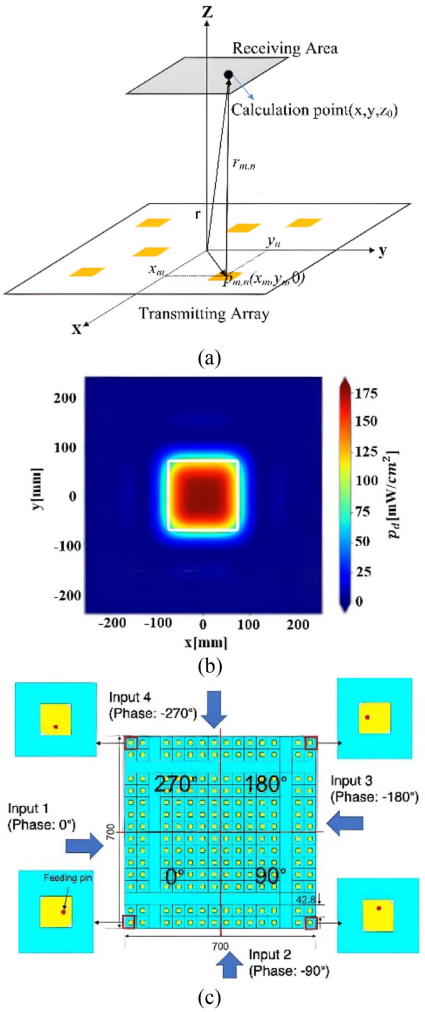

FIGURE 5. Flattop beam generation. (a) Coordinates and antenna. (b) Flat top beam pattern. (c) Proposed block-oriented sequential array method [46].

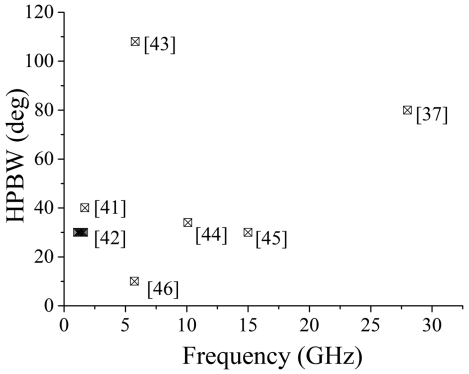

FIGURE 6. HPBW comparison of the preceding flattop antennas.

design simplicity, the whole phased array with 196-element microstrip antennas is subdivided into four 49-element blocks, and each block was rotated counterclockwise by 90° to realize block-oriented sequential array excitation for flattop beam, as shown in Fig. 7(c).

The recent design methods for generating flat-top beam are summarized in Table 2, where the uniform radiation pattern is satisfied in a certain angle range, as displayed in Fig. 6, and the sidelobes are deigned to be very low for engineering applications. It is worth noting that the efficiency for flat top beam is not high. Even with 196-element antenna array, the beamwidth of the proposed flat top beam is still wide. Due to the wide beamwidth, the energy is largely scattered in open space or wasted at unused areas, resulting in low beam utilization efficiency. Hence, the power transfer efficiency of the flat-top beam would be not better than that of a conventional -3 dB beam.

C. NON-DIFFRACTIVE BEAM

Non-diffractive beam, whose energy is not diffracted within the transmission distance, has an important application value for near-field microwave power transmission. Due to non-diffractive characteristics, the electromagnetic wave can reach the target through space to achieve energy non-diffusion, thereby improving the electromagnetic wave transmission efficiency.

Many types of non-diffractive beams exist, such as the Bessel wave, Caleidoscopic wave, Mathieu wave, and Vortex wave. Compared with other non-diffractive beams, Bessel beams possess potential application value in microwave energy transmission, due to good lateral resolution, narrow intensity profiles, and high directivity [47]. First proposed in 1987, Durnin et al. obtained the nonsingular solutions of the scalar-wave equation for zero-order Bessel beams in free space, which is non-diffractive beams. Unlike the plane waves, the ideal Bessel beam possesses an infinite depth of field [49]. For physically realizable finite-aperture, the pseudo-Bessel beam with a finite transverse size has a finite amount of energy. Along its propagation direction, the main lobe does not expand until the Rayleigh distance, which is the

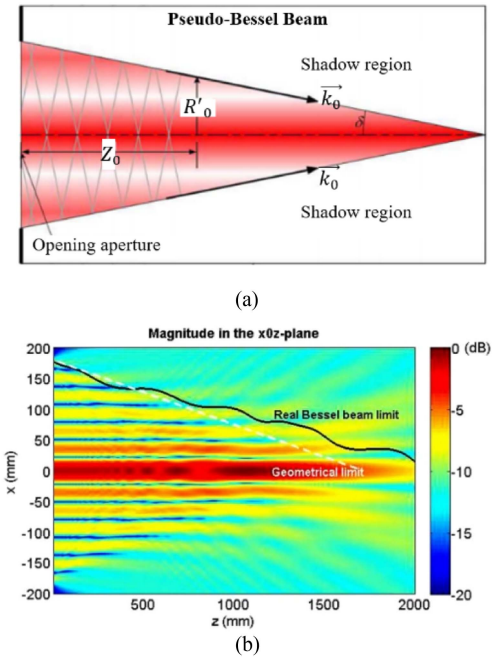

FIGURE 7. Non-diffractive beam. (a) Pseudo-Bessel beam generated by the infinite antenna aperture, where the aperture radius R_0, the axicon angle δ, the wavenumber vector k_0. (b) Pseudo-Bessel beam along the non-diffractive distance [50].

non-diffractive distance. Within the non-diffractive distance, the beam maintains the non-diffractive behavior over long distances even truncated, as displayed in Fig. 7(a), while over non-diffractive distance, Bessel beam diverges inevitably. The outermost lobe will diverge first and the beams inside diverges successively, until the main lobe finally diverges, as shown in Fig. 7(b) [50]. In this article, the pseudo-Bessel beams is referred to as the non-diffractive beam.

Initially, non-diffractive beams were widely used in the optical field, and many methods for generating non-diffractive beams have been proposed in optics, such as the computational holography, the axial cone lens, the resonant cavity and the spherical aberration [51]. For high transmission efficiency in microwave power transmission, the non-diffractive beam generation techniques extend from optics to the microwaves. The main idea of these non-diffractive antenna designs is to achieve large depth of field, compact size, and low sidelobes.

In [50], two-dimensional antenna arrays were proposed for nondiffractive beam generation by using sub-sampled distributions, as shown in Fig. 8. The Bessel beam is synthesized with an analytical method based on a least mean square error minimization, where the beam function obtained by the array with optimal excitation is not dramatically different from the target function. It is found that the non-diffractive beam with low amplitude oscillations can be demonstrated over distances of about 300 λ_0, where λ_0 is wavenumber in vacuum. However, the proposed antenna array was electrically large for propagating over long distance. Besides, different amplitude and phase excitations are required for the arrays, resulting in complicated feeding networks.

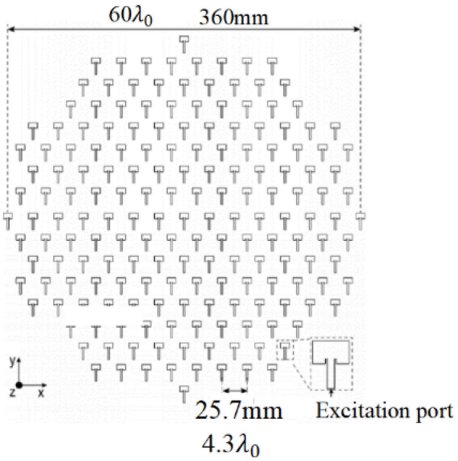

(a)

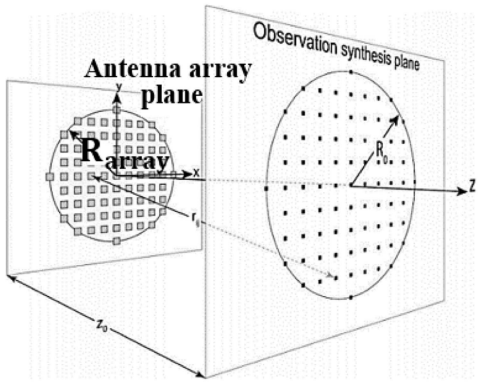

(b)

FIGURE 8. Non-diffractive beam generation. (a) Two-dimensional antenna arrays with spacings of approximately $4\lambda_0$. (b) Least mean square synthesis technique [50].

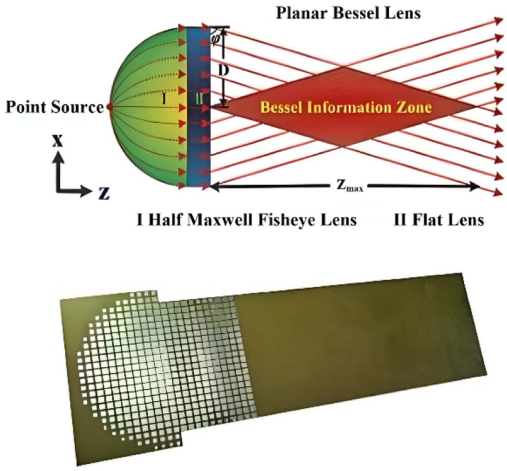

FIGURE 9. Surface-wave Bessel lens [61].

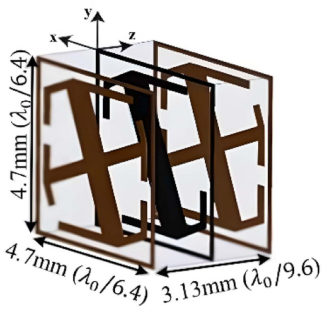

(a)

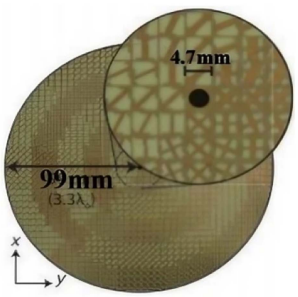

(b)

FIGURE 10. Phase shifting surface antenna for non-diffractive beam [56]. (a) Phase shifting element. (b) Phase shifting surface array.

In recent years, metamaterials, acting like a converter, have been widely used to generate the nondiffractive beam due to its excellent capability of manipulating electromagnetic waves [56]. To simplify the feed network, a gradient index (GRIN) metamaterial lens with a waveguide antenna was proposed for generating non-diffractive beams. By using the metamaterial lens, the spherical beam emitted from feed is transmitted into conical beam, and accordingly the conical beam forms nondiffractive beam in the near-field zone [60]. Due to their simple structure and easy processing the metasurfaces, i.e., a two-dimensional form of metamaterials, has attracted plenty of attentions.

In 2014, a planar metasurface lens consisting of a half Maxwell fisheye lens and an inhomogeneous flat lens was proposed to produce nondiffractive surface waves. Through the planar metasurface lens, a point source on the fisheye lens directly excites the non-diffraction surface waves, as shown in Fig. 9 [61]. In the same year, the vector nondiffractive beam was manipulated by the non-reflective metasurfaces, which realizes amazing electromagnetic wave front control. Since the metasurfaces can efficiently control the polarization and phase, the arbitrarily polarized Gaussian beams are developed into vector non-diffractive beams by using metasurfaces, as displayed in Fig. 10 [56].

To expand the bandwidth, a wideband Phase Shifting Surface (PSS) antenna is presented for large non diffractive range with stable beam intensity. To generate the required non-diffractive beam, multilayer metallic square patches are used to adjust the phase distribution on the PPS aperture [62]. In addition to the transmission metamaterials /metasurfaces,

(a)

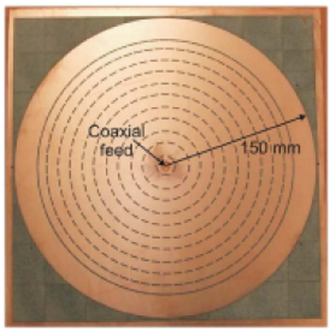

(b)

FIGURE 11. RLSA structures. (a) Proposed in [64]. (b) Designed in [65].

non-diffractive beams have been designed by using reflective metasurfaces. In [63], a reflective metasurface array with artificial admittance modulation surface is proposed to construct a nondiffractive beam. These designs demonstrate that the electromagnetic waves are successfully modulated, and good performance of non-diffractive beams can be obtained by using metamaterials and metasurfaces.

A main problem of the metamaterials/metasurfaces lens is that the feed position is required to be at the focal point for non-diffractive beam, and integrating the feeding antenna with the lens is difficult. Radial Line Slot Antenna (RLSAs) were reported addressing such problems [64], [65], [66], [67], [68], [69]. For example, an efficient non-diffractive beam with high polarization purity is propagated by using a RLSA structure, which is manufactured in the radiating slots array plate and the background plate of the parallel planar waveguide. By using a holographic approach, the desired aperture field distribution is assured, and the antenna slot layout is optimized, as displayed in Fig. 11(a) [64]. Another design was reported to launch Bessel beam by using a finite inward Hankel travelling wave. The desired distribution is defined over the RLSA aperture to launch a nondiffractive beam [65], [66]. Based on the holographic approach, an optimization procedure is used for adjusting the slots position and slots size on the RLSA aperture, as displayed in Fig. 11(b) [65]. These non-diffractive beam launchers are proposed with the scalar theory, leading to large aperture size and wide beam width.

To achieve a narrower beamwidth, a vector method with the derived boundary conditions is used rather than the scalar method [67]. Some preliminary studies have investigated the novel non-diffractive beams with the benefits of guided mode or leaky-wave mode [67], [70]. Generation of transverse electric (TE)/transverse magnetic (TM)-polarized nondiffractive beams was proposed by using a leaky radial waveguide. The antenna consists of an inductive/capacitive sheet over a ground plane, and then supports the leaky-wave mode for non-diffractive beam generation [69], [70]. However, the non-diffractive beams launched by those structures are azimuthally invariant, and always perpendicular to the aperture.

For multiple targets or the moving target, the non-diffractive launchers should be rotated to track the targeting locations. For the fixed structures, the direction of the non-diffractive beam should be manipulated. Recently, a reconfigurable non-diffractive antenna was proposed for near-field beam scanning. By selectively switching the states of PIN diodes in different regions by turns, diverse wavenumbers against azimuths were excited, thus the near-field beam was deflected in different zones [71]. However, the additional loss would be introduced by the PIN diodes, and the field intensity decreases dramatically. To improve the field intensity, a leaky wave antenna structure was warped for the inclined non-diffractive beam rather than the lossy components [72]. To achieve the curved structure, the sophisticated processing was needed. To avoid the non-planar manufacture, the metasurface lenses were designed. In [73], a coding metasurface was formed by alternately stacking three metal patches and four polyimide spacers to realize a perpendicular or an oblique non-diffractive beam. Thereafter, a wide band phase shift surface antenna was designed to generate the non-diffractive beam with adjustable depth-of-field at different titled angles [74]. Nevertheless, a multi-layer metasurface unit was designed, which owned high antenna profile. To achieve low profile, a monolayer reflective metasurface was proposed to realize the nondiffractive beam manipulation. Then, by using the Risley prisms, the Phase Shift Surfaces (PSS) were proposed to achieve two-dimensional scanning of non-diffractive beam, as displayed in Fig. 12, where the non-diffractive beam can be steered by mechanically rotating two PSSs within the anterior hemisphere of the antenna. Nevertheless, two phase shift surfaces still increased the entire antenna profiles [75]. Subsequently, a single-layer metasurfaces, e.g., reflective metasurfaces [63], asymmetric gradient refractive index metasurfaces [76] and grapheme-based metasurfaces [77], was proposed to realize non-diffractive beam scanning. By changing the operation frequency [63], [76] or designing different metasurface planes [77], the inclined non-diffractive beam could be realized at different tilted angles.

Furthermore, the key performance metrics, namely the maximum nondiffractive distance and tilted angle, are presented in Fig. 13. It is evident that the nondiffractive distance is relatively limited, with a maximum achievable separation of only 25 wavelengths. Similarly, the deflection angle is constrained, with a maximum tilted angle of 54°. The performance of the non-diffractive launchers for the inclined beam is compared, as listed in Table 3. It can be seen that the

TABLE 3. Performance of the Preceding Designs for Inclined Non-Diffractive Beams at Microwave and THz Frequencies

Ref.	Center frequency	Structure (Design complex)	Size (mm^3)	Maximum nondiffractive distance	Maximum tilted angle (°) for beam deflection
[63]	15 GHz	Reflective metasurface (Simple)	200 × 200 × 150 ($10\lambda_0 \times 10\lambda_0 \times 7.5\lambda_0$)	400 mm ($20\lambda_0$)	12
[71]	10 GHz	Reconfigurable leaky wave antenna (Moderate)	$1 \times 88.89^2 \times \pi$ ($0.1\lambda_0 \times 2.96\lambda_0 \times 2.96\lambda_0$)	63.5 mm ($2.11\lambda_0$)	16.2
[72]	36 GHz	Curved substrate integrated waveguide (Complex)	-	90 mm ($10.8\lambda_0$)	18
[73]	1 THz	Coding metasurfaces (Complex)	3.3×3.3×0.085 ($11\lambda_0 \times 11\lambda_0 \times 0.28\lambda_0$)	1 mm ($3.33\lambda_0$)	32
[74]	29 GHz	Phase shift surfaces (Simple)	$173.6 \times 100^2 \times \pi$ ($17.4\lambda_0 \times 17.13\lambda_0 \times 17.13\lambda_0$)	200 mm ($20\lambda_0$)	30
[75]	29 GHz	Two phase shift surfaces (Moderate)	$186.5 \times 100^2 \times \pi$ ($18.1\lambda_0 \times 17.13\lambda_0 \times 17.13\lambda_0$)	256 mm ($25.6\lambda_0$)	54
[76]	10 GHz	Gradient refractive index metasurfaces (Simple)	86.5×80×1.6 ($2.88\lambda_0 \times 2.67\lambda_0 \times 0.05\lambda_0$)	66.1 mm ($2.2\lambda_0$)	14.5
[77]	1.5 THz	Graphene-based metasurface (Complex)	1.6×1.6×0.025 ($8.12\lambda_0 \times 8.12\lambda_0 \times 0.13\lambda_0$)	2.612 mm ($13.27\lambda_0$)	15

nondiffractive transmission distance is comparable and relative to the antenna aperture. The longer the nondiffractive distance, the larger the aperture size, since the aperture's physical dimension is proportional to the nondiffractive distance. For the remote targets, the beam energy almost keeps constant along the nondiffractive distance, and the target can be wirelessly charged without substantial decrease in transmission efficiency along the transmission direction. Though the nondiffractive beams overcome the weakness of focused beam control to some extent, these non-diffractive antennas have not been widely used in practical engineering. That's because high sidelobes are one of the main factors which leads to low power transmission efficiency on its main beam direction.

D. SUPERGAIN/SUPERDIRECTIVE BEAM

Conventionally, antenna gain is affected by the antenna aperture, which can be expressed by

$$G \leq (2\pi R_e)^2 + 2\,(2\pi R_e)\,, \quad R_e = R/\lambda \tag{1}$$

where R/λ is maximum electrical dimension of the antenna, i.e., the ratio of antenna dimension to wavelength.

To break through the upper limit of the theoretical gain of the antenna, the supergain is defined by [78],

$$G > (2\pi R_e)^2 \tag{2}$$

For high transmission efficiency, the supergain/superdirective antennas, whose directivity/gain is higher than the typical gain with the same physical size, are proposed. To obtain significant superdirectivity, the accuracy of the amplitude and phase of the excitation current needs to be rapidly improved. Uzkov et al. [79] demonstrated that the linear array composed of N isotropic elements could achieve the maximum directivity of N^2 in the end-fire direction in principle.

To mitigate the limitations, much work has been done, most of which are related to monopole and dipole antennas. In [80], two closely spaced bow-tie monopoles fed by a power divider were proposed with a matching network and a decoupling network, as presented in Fig. 14(a). In addition to the matching network, the amplitude and phase of the current are excited for each antenna element to achieve high accuracy requirement with the decoupling network. However, the array operates at very narrow band, and the antenna robustness is poor. For a wider frequency bandwidth, a two-element superdirective array composed of wideband planar plate monopoles is shown in Fig. 14(b), where a pair of small rectangular parallel plates is attached to the radiating edges of the monopole for further expanding the frequency band [81].

To simplify the feeding network, a parasitic array is used rather than a separate feeding network which requires a large area. For the parasitically loaded array, the current excitation coefficients with the input impedance matrix were deduced for the required loads based on Yaghjian method [82]. In [83], the four-element superdirective array was designed based on folded meandered dipole, and the array was composed of a single active and three parasitic elements with optimal impedance loads for good matching. Electrically small antenna parasitic arrays are amongst the most popular structures for superdirectivity [84], [85], [86], [87], [88], [89], [90]. Among them, a superdirective array composed of closely spaced electrically small resonant elements was proposed based on the Yagi-Uda principle, as displayed in Fig. 15 [84]. For miniaturization, an electrically small antenna design, inspired by metamaterials was presented, as displayed in Fig. 15(b) [85] and (c) [86]. Due to the metamaterial-inspired

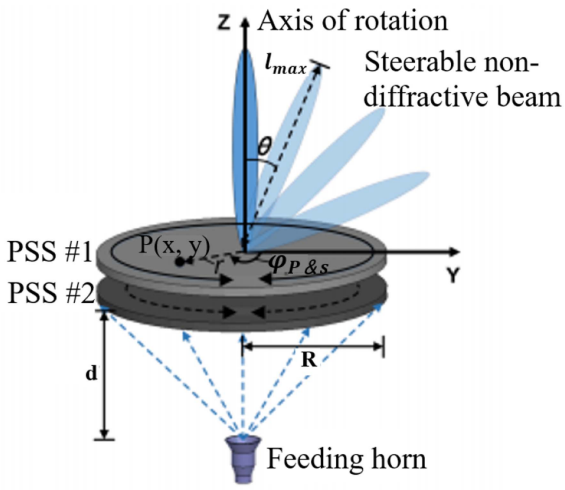

(a)

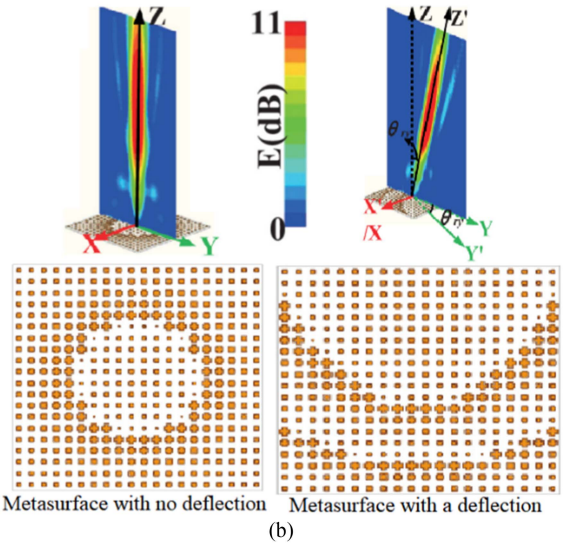

(b)

FIGURE 12. Diagrammatic sketch of the steerable non-diffractive beam. (a) Non-diffractive beam launched by two PSSs [74]. (b) Graphene-based metasurfaces with/without deflection [76].

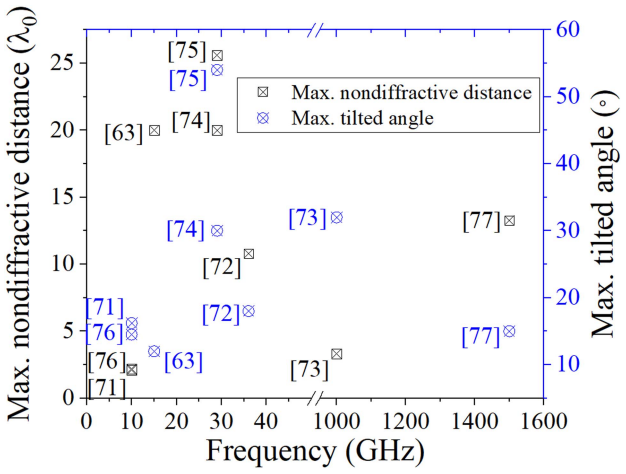

FIGURE 13. Maximum nondiffractive distance and tilted angle of the recent works.

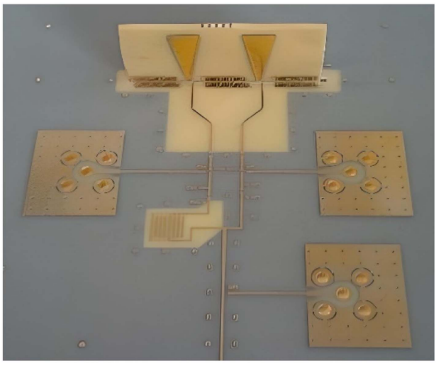

(a)

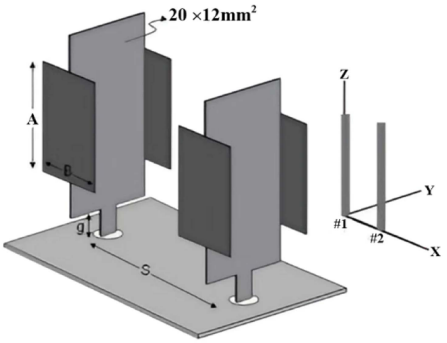

(b)

FIGURE 14. Superdirectivity array. (a) Fed by a power divider associated to a matching network and a decoupling network [80]. (b) Wideband planar plate monopole array with two loading parallel plates [81].

structure, a high directivity and compact size can be achieved by using electrically small monopole. The state-of-the-art antenna designs proposed for achieving high directivity are compared in Fig. 17. While these antennas achieve high directivity, their total efficiency is often low, resulting in low antenna gain. This low efficiency can be attributed to the high power dissipation caused by the surface resistance of the materials used in these antennas. Therefore, these antennas are primarily designed for high directivity rather than high gain. The detailed antenna performance parameters are provided in Table 4, which highlights that monopole, electrically small resonant, and metamaterial architectures are commonly accepted approaches for achieving superdirectivity antennas, particularly due to their compactness.

To address the low-efficiency problem, matching networks with enhanced decoupling and isolation [91] and conformal structures [92] were employed to improve antenna efficiency from an impedance matching perspective. Alternatively, superconductor instead of traditional metal material (e.g., copper) is used to improve the intrinsic low antenna efficiency. To achieve the supergain, the closely spaced printed dipole array made of high-Tc superconductors (HTS), e.g., thick film YBCO [93] or thick film YBa2Cu3O7-x [94] was designed, as

TABLE 4. Performance of State-of-the-Art Antennas Designed for Superdirectivity

Ref.	Frequency (MHz)	Size (mm^3)	Directivity (dBi)	Antenna efficiency (%)	Structure (Design complexity)	Applications
[80]	5500	-	9.51	34.4	Monopole array with matching network and decoupling network (Complex)	Single target or unmovable target
[81]	3100	20×12×21 ($0.37\lambda_0\times0.22\lambda_0\times0.385\lambda_0$)	9.5	60	Monopole array with power divider and phase shifter (Moderate)	
[82]	866	110×70×0.8 ($0.32\lambda_0\times0.2\lambda_0\times0.002\lambda_0$)	7.2	62	Microstrip parasitic array (Simple)	
[83]	861	231.46×99.06×1.524 ($0.66\lambda_0\times0.28\lambda_0\times0.004\lambda_0$)	10	8.3	Folded meandered dipole (Simple)	
[84]	435	130×190×1.524 ($0.19\lambda_0\times0.28\lambda_0\times0.002\lambda_0$)	9.9	55	Electrically small resonant rings array (Simple)	
[85]	1820	45×27×0.8 ($0.27\lambda_0\times0.16\lambda_0\times0.005\lambda_0$)	7.2	70	Metamaterials (Simple)	
[86]	1017	50×50×8.524 ($0.17\lambda_0\times0.17\lambda_0\times0.029\lambda_0$)	5.18	4.2	Metamaterials (Simple)	
[87]	905	54×24×0.76 ($0.16\lambda_0\times0.07\lambda_0\times0.002\lambda_0$)	7	7.1	Microstrip parasitic array (Simple)	
[88]	866	110×107×0.8 ($0.32\lambda_0\times0.31\lambda_0\times0.002\lambda_0$)	9.2	11.2	Microstrip parasitic array (Simple)	
[89]	728	110×70×0.762 ($0.27\lambda_0\times0.17\lambda_0\times0.0018\lambda_0$)	2.5	20	Metamaterials (Simple)	
[90]	2480	60×60×10.3 ($0.5\lambda_0\times0.5\lambda_0\times0.085\lambda_0$)	5.7	40	Metamaterials (Simple)	

shown in Fig. 16. In [93], integrated to a feeding network with a balun, a sixteen-element superconducting array was demonstrated for high gain, which is obviously higher than that of a similar supercooled silver array, albeit at the cost of narrow bandwidth. In [94], in terms of the performance of printed dipole arrays, i.e., efficiency and bandwidth, the basic feeding configurations were explored to induce the desired superdirective excitation, and a corporate fed HTS array of four dipoles was characterized for the supergain. Even though the superconductivity property of HTS can be achieved with low-cost liquid nitrogen (the temperature is less than 77 K), challenges arise in the packaging and fabrication of the antenna, which must be resolved in practical applications. Besides, the bandwidth of supergain/superdirectivity antenna remains very narrow.

E. FOCUSED BEAM

To improve the system efficiency, alternative technique is to focus the radiated energy at the receiving antenna location for high gain with narrow beams and low sidelobes. To realize near-field focusing, the synthesis methods for near-field focusing beams mainly including conjugate-phase method, optimization-based method have been proposed, and the maximum power density is achieved at the focal point for high transmission efficiency. For near-field focusing on a single focal point, the most basic and common method is conjugate-phase method [95]. The equivalent model for near-field focusing can be obtained by using ray-optics approximations, as shown in Fig. 18. The basic concept is to control the phase of the sources on the aperture (the currents of the array element or equivalent aperture surface), so that the phases are added at a specific focal point in the near-field region.

Near-field focusing antennas are designed based on parameters such as operating frequency (or free-space wavelength), and focal length R_f. According to Fig. 18, the phase distribution of the aperture can be calculated using the conjugate-phase method, as expressed by [95],

$$\phi(x, y) = (2\pi/\lambda)\left[\sqrt{(x^2 + y^2 + R_f^2)} - R_f\right] \tag{3}$$

where λ represents the free-space wavelength at the operation frequency. To implement a near-field focus, when propagation from the sources, the waves are gathered at a focused point with an equal-phase superposition. By using the conjugate-phase method, the traditional optical-focusing structures, i.e., horn lens antenna, reflectarray, reflector antennas and the phased array antennas have been proposed, as displayed in Fig. 19. The use of a lens to focus a beam has been studied in several references [96], [100], such as a metal plate lens [96], [97] and a dielectric lens [98], [99], [100], [101]. To achieve the focus beam, the dielectric lens should be placed in front of the horn [98] or inserted into the horn [99], [100], [101]. A double-reflector beaming experiment over a 7.62 m range achieved a 63.7% beam efficiency based on a quasi-optic approach [102].

An alternative implementation for a near-field focused radiation is the reflectarray [103], [104], [105], [106]. A reflectarray consists of reflecting surface and a feed. To achieve focusing beam, the microstrip patches are used as reflecting

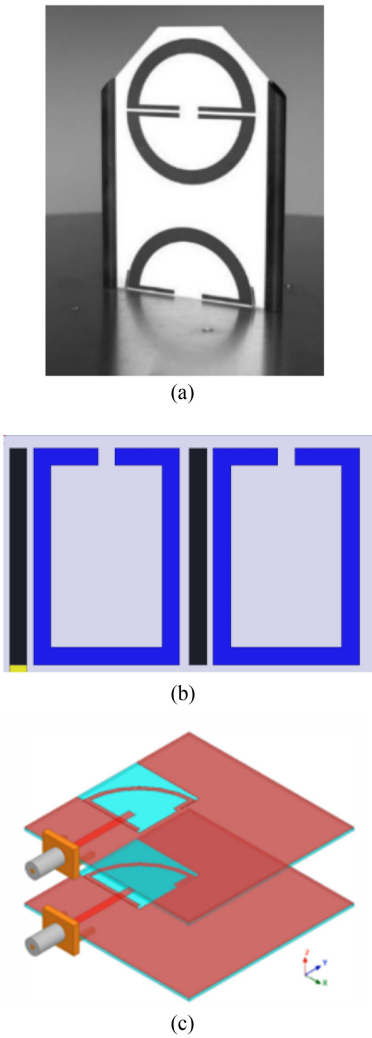

FIGURE 15. Superdirective array composed of electrically small antenna parasitic arrays. (a) Small resonant magnetic dipole array [84]. (b) Metamaterial-inspired electrically small antenna array [85]. (c) Metamaterial-inspired electrically small antenna array [86].

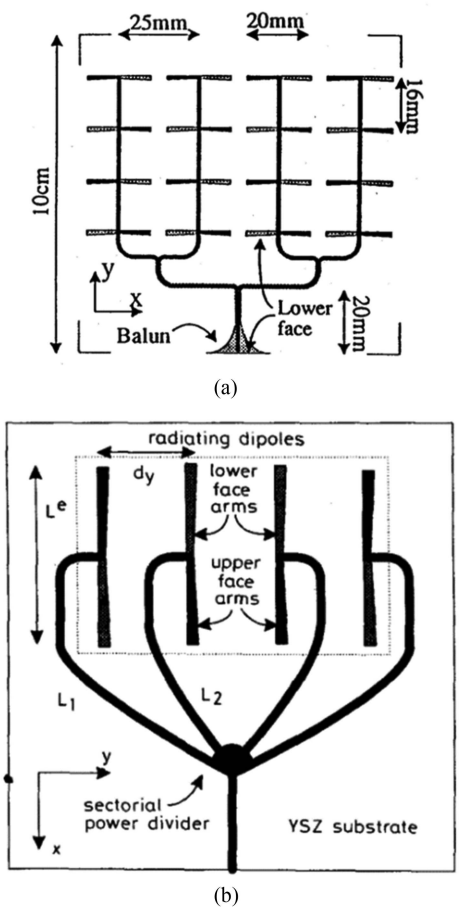

FIGURE 16. Superconducting supergain array. (a) A sixteen-element superconducting printed dipole array [93]. (b) A corporate fed HTS array [94].

elements, whose phases are varied by changing the patch sizes. The phase of the field has to be adjusted along the antenna aperture to obtain a locally plane wavefront at a focal point. Reflectarrays have also been reported on low-cost foldable materials such as e-textiles, enabling rapid deployment of focused WPT [107].

Similar to the reflectarray, the reflectors with various shapes have been proposed. For example, an elliptic reflector antenna is considered due to its dual-focus nature, which allows for the fields radiated by a focus feed is illuminated to the reflector and then the equal-phase scattering fields is produced at the other focus [107]. In addition to the elliptic reflector antenna, the prolate-spheroidal reflector antennas [109] and the dome-shaped ellipsoidal antennas [110] were designed based on the dual-focus feature of the geometry itself in the near-field region. Since the feed is located at either side of the two foci can create a focused beam around the other foci, an axial energy focusing is formed, where the energy is not only confined in a limited area (near-field beam focusing), also the interference effect is minimized beyond the targeted area. However, these antennas are usually bulky, expensive, and difficult to manufacture. To facilitate scalable manufacturing and integration, lightweight and low-profile focused structures can be obtained by using antenna arrays. By implementing feedline with different length, each source on the aperture has a different distance from the focus, which could be able to compensate for a symmetric source-phase tapering to generate the focus beam. The performance of the near field focusing array, i.e., focal distance and focal size, mainly depends on the number of elements, the element spacing and the operating frequency. To achieve good focus property, a special form of antenna array, i.e., multifaceted antenna array [111], [112] is arranged in a cylindrical configuration. Due to the cylindrical arrangement, a linear planar array would concentrate the radiation fields at the circle center formed by the panels. However, the extra feedlines of the antenna array would introduce large loss, causing low power transfer efficiency.

The conjugate-phase method is simple and efficient for single-focus problem, while the optimization-based synthesis

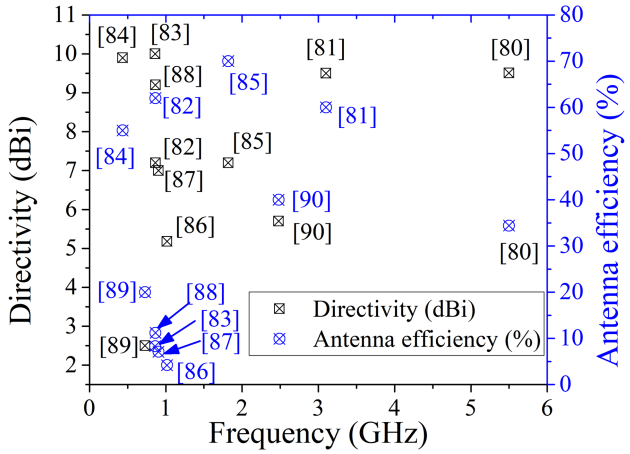

FIGURE 17. Directivity and antenna efficiency of the state-of-the-art superdirective antennas.

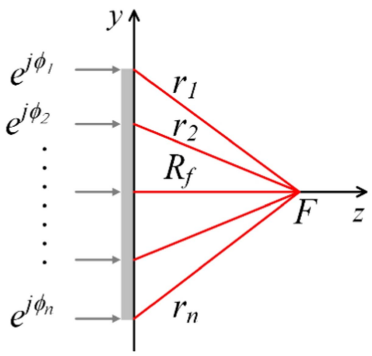

FIGURE 18. Schematic representation of an equivalent model, where F is the focal point, r is the distance between the focal point and the aperture, ϕ is the phase of the radiation sources.

method is a particularly suitable for multi-point focusing and 3D focal spot shaping. Shaping near field focusing beam is a nonlinear three-dimensional problem due to the nonlinear spatial phase factor between aperture sources. To optimize the focusing characteristics, different approaches have been presented, such as the steepest descent method [113] and Levenberg–Marquardt algorithm [114]. In the optimization-based process, the amplitude and phase of the antenna sources can be determined by minimizing a properly defined objective function to improve the focusing property for the multiply targets. For example, based on the iterative Levenberg-Marquardt (LM) algorithm, Álvarez proposed an optimization method to reduce the sidelobes level around the focal region and the focus shift [114]. In [115], Wu proposed a machine learning method to predict the amplitude and phase of the near field focusing phased array to achieve beam scanning and polarization manipulating.

Based on multi-task Bayesian compressed sensing (MT-BCS) method, Huang proposed a synthesizing process for near field focusing by using sparse antenna arrays. By optimizing the excitation of the array, the optimal line array can save more than 30% of the number of array elements compared with the equidistant linear array, and the optimal planar array can save more than 50% of the number of array elements compared with the equidistant planar array [116]. Most synthesis techniques for near field focusing only consider the relative position between the radiating sources and the focal spot, while ignoring other interferences on the power transmission efficiency from other directions in the nearby environment. Thus, a scheme for near field focusing synthesis was reported to be extended to constrains in the far field radiation patterns [117]. Weights optimization applied to an antenna array is one of the most flexible ways in near field focusing synthesis [118], the proposed technique allows a predefined near field focusing while minimizing the far field pattern.

The focal length of state-of-the-art focusing antenna designs is compared in Fig. 20, revealing that the focal length is remarkably short, typically spanning just a few wavelengths. With the aid of advanced algorithms, such as tuning the aperture angle or element phase, the focal spot can be continuously adjusted, offering flexibility and adaptability in the focusing capabilities of the antenna. Besides, other performance metrics are listed in Table 5. It can be seen that the focus length in the near-field is closely related to the aperture size, and they tend to be positively correlated. Similar to nondiffractive beam, the transmission distance is comparable to the antenna aperture. Conventionally, the focus control is not easy, the phase of the radiation sources should be adjusted for the focus property control. Even with an optimization-based synthesis method, the phase array requires a large number of expensive phase shifters for the phase manipulation. Accordingly, the feeding network of the phase array is complicated, high-lossy and hard to power transmission.

E. TIME REVERSAL

With traditional near-field focusing methods, it is difficult to realize automated tracking of the moving target. To address this problem, Retro-Directive Wireless Power Transfer (RD-WPT) provides an efficient approach [119], [120], [121]. Besides RD-WPT, methods like time reversal (TR) [122], [123] and backscatter [124] can allow the transmitter system toto adaptively position and track the mobile devices without any auxiliary positioning equipment. Among them, the positioning accuracy by using TR technology in complicated scattering environments (i.e., indoor environment and a fully shielded metal cavity) usually exhibits much higher. The basic principle of the TR technique with adaptive focusing is that the signal is reversed in the time domain or conjugated in the frequency domain, and the signal will be focused at the same point at the same time instance [126], as displayed in Fig. 21, where the wave equation with second-order derivative to time has the time reversal invariance. Time Reversal Mirror (TRM) used as one of the most important components is the temporal correlation of the incident field emitted by the source is recorded on each transceiver, which then plays back

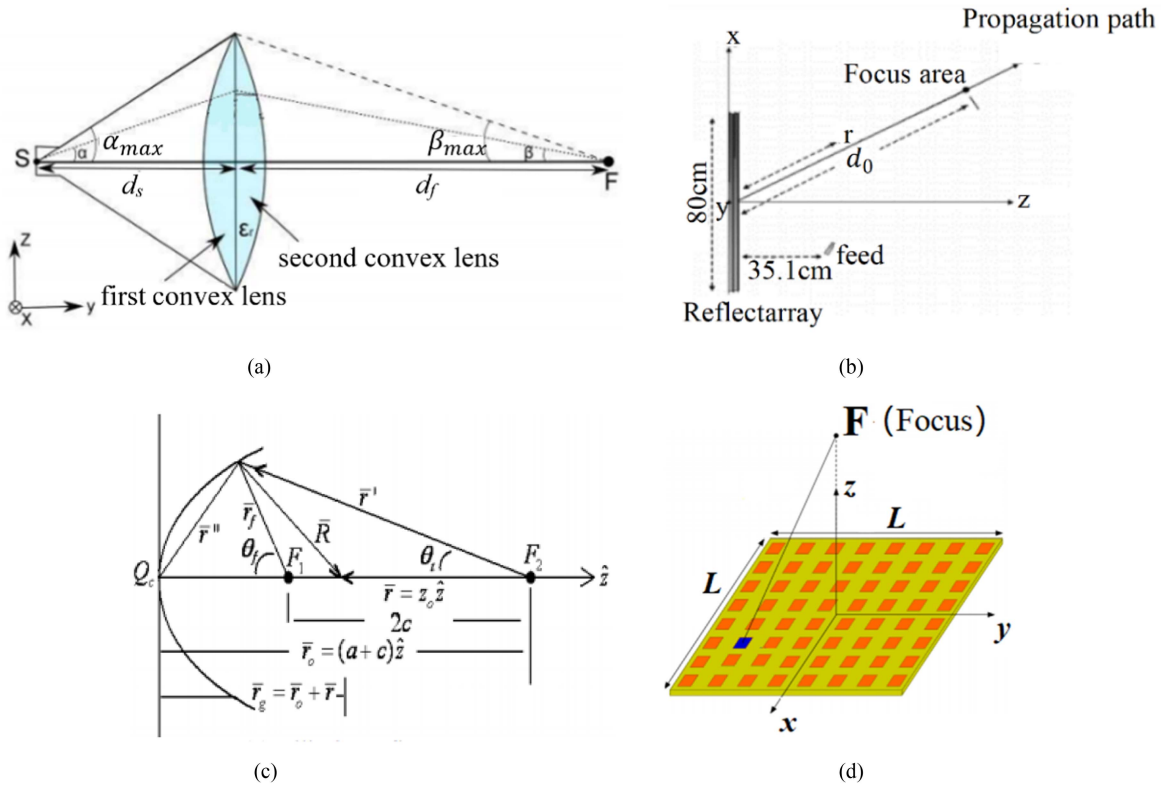

FIGURE 19. Focused antenna structures. (a) Lens antenna. (b) Reflectarray. (c) Reflector antenna. (d) Antenna array.

TABLE 5. Performance of Different Near-Field Focusing Antennas

Ref.	Antenna type	Freq. (GHz)	Aperture geometry and size	Focal length (R_f)	Focal spot for applications	Design method (Design complex)
[96]	Metal plate lens antenna	9	Linear array, length = $7.2\lambda_0$	$7.5\lambda_0$	Fixed spot for single target or unmovable target	Conjugate-phase method (Simple)
[104]	Planar reflectarray antenna with two feeds	2.45	Square, $10.8\lambda_0\times10.8\lambda_0$	$8.2\lambda_0$	Fixed spot for single target or unmovable target	Conjugate-phase method with correction terms (Moderate)
[105]	Patch reflectarray antenna	5.8	Square, $8.7\lambda_0\times8.7\lambda_0$	$10\lambda_0$	Fixed spot for single target or unmovable target	Conjugate-phase method (Simple)
[112]	Corner-reflector-like phased array	2.4	Corner-reflector-like geometry, $1.5\lambda_0\times4\lambda_0\times0.86\lambda_0$	$4\lambda_0$~$7.2\lambda_0$	Tunable spot for multi-target or moving target	Shaping the 3D focal spot by tuning the aperture angle (Complex)
[115]	FPGA-controlled phased array	2.45	Square, 256 elements	$6\lambda_0$	Tunable spot (focal spot shape scanning and polarization manipulating) for multi-target or moving target	Support vector machine (SVM) algorithm (Complex)
[118]	Microstrip phased array	12	Square, $6.4\lambda_0\times6.4\lambda_0$	$4.8\lambda_0$~$6.4\lambda_0$	Tunable spot for multi-target or moving target	Levenberg-Marquardt (LM) algorithm (Moderate)

the signal in reverse order. Thus, in free space, the inverse-propagating wave focusing on the source location.

The adaptive spatial temporal focusing of TR was firstly reported in acoustic field by Fink [127], and executed subsequently by Lerosey in microwaves [128]. TR technology is proposed as a promising alternative to the energy focus. While extensive prior researches about the electromagnetic TR exist [128], [129], [130], [131], [132], they remain largely unexplored on the field of wireless power transmission. Considering the complex environment, transmission efficiency of the transmitters and receivers declines rapidly due to the multipath effect, while the adaptive focusing technology, i.e.,

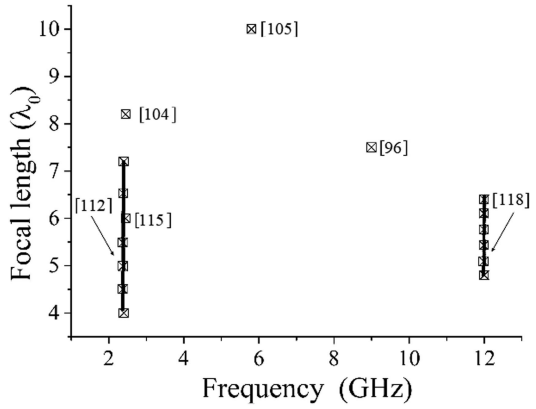

FIGURE 20. Focusing length comparison of the published works.

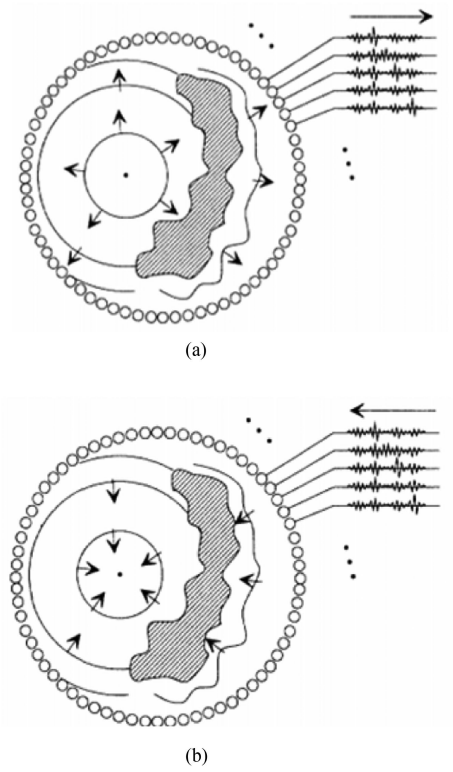

FIGURE 21. Time reversal technology. (a) First step of TR process: Recording. (b) Second step of the TR process: Reconstruction.

time reversal technology can adaptively focus on and enhance the field intensity on the receiver. Due to the characteristic of TR, the interference of electromagnetic wave propagation trends to be effectively minimized, as is multipath delay attenuation. Thus, TR used for wireless power transmission, i.e., TR-WPT has been developed. Recently, a spatial focusing system consisting of a single transmitting antenna and a single receive antenna has been implemented. The electromagnetic energy is accurately delivered to the target point in the way of "point focused wave", as displayed in Fig. 22(a), which has the advantages of high energy transmission efficiency, large

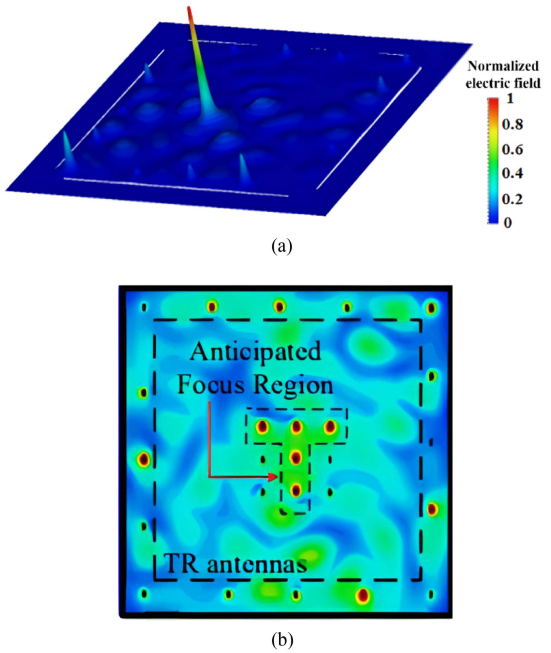

FIGURE 22. Focusing beams. (a) Single point focusing [132]. (b) Multi-point focusing [133].

energy transmission range, and flexible energy transmission control [132].

In addition to a single point focus, TR technology has a great potential to adaptively focus power on the multi-targets, where the non-battery powered devices are located. In [133], a multi-target TR approach was optimized to improve computational efficiency, depending on the temporal excitation synthesis of TRM, as displayed in Fig. 22(b). Another possible strength of TR-WPT is that multi-users can simultaneously supply wireless power [134], [135]. The multi-user power transfer is considered to generate a plurality of TR single-point focusing fields in the power transmission area, and each single-point focusing field provides power to one user. Based on the one-point TR scheme, the multi-target TR-WPT system performs in the synchronous focus mode. The received power is in inverse proportion to the propagation attenuations relative to the transmitters, e.g., a user closer to the transmitters receives more power, while the user farther away from the transmitters receives less power. These studies reveal the capability of TR to control waves and focus energy in complex media, containing multipath and multi-reflection. Compared to beamforming at the same average transmitting power, TR achieves higher peak voltages at the receiver in an indoor multipath environment [136]. Particularly in complex multipath environments, i.e., aircraft cabin or indoor room, TR can make full use of rich multipath to provide more power at the target zones [134].

To facilitate the focusing property control, TR technology with adaptive focusing feature is a good candidate for multi-target and moving target. However, the complex multipath environment, i.e., indoor and metal chamber is provided to

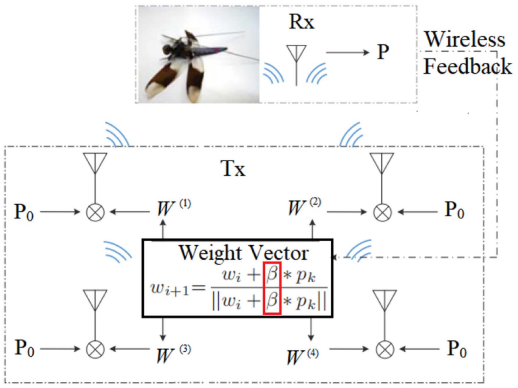

FIGURE 23. Far-field wireless power transfer towards moving object proposed in [137].

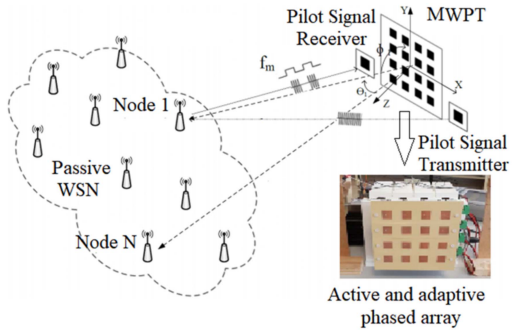

FIGURE 24. Representation of the proposed WPT system for PWSNs [124].

achieve good focusing characteristics, either single point or multi-point focus. Besides, a number of the time-reversal mirrors are located around receiving antenna.

F. ADAPTIVE BEAMFORMING TECHNIQUE

Besides near-field focusing methods, several adaptive beamforming techniques have been proposed for MWPT, particularly in multipath environments. In [137], a fast-beamforming WPT technique is introduced for moving targets. By dynamically adjusting the perturbation factor β during the powering-up process, the transmitter power can be optimized in a shorter time. The scheme for far-field wireless power transfer towards moving objects is illustrated in Fig. 23. For multiple targets, an active and electronically steerable phased array is employed to select, track, and wirelessly power passive wireless sensor network (PWSN) nodes within a specific area, as depicted in Fig. 24. Based on the received signal strength of each node, a specific amount of power is configured for optimal power transmission [124].

In wireless sensor networks, the allocation of transmitters and receivers significantly impacts power transmission performance. In [138], transmitter and receiver locations are jointly optimized using adaptive magnetic beamforming, maximizing the power delivered to the receiver over a target region. In [139], a buffer-aided adaptive wireless-powered communication network is proposed. The work considers energy beamforming, optimal power allocations, rate control, time

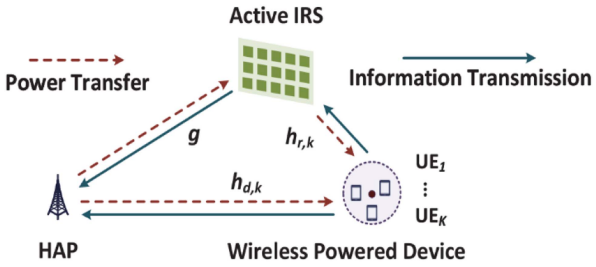

FIGURE 25. An active IRS-aided WPCN [145].

allocations, and transmission mode selection with a weighted max-min fair access scheme. Channel state information (CSI) is crucial for energy beamforming; however, due to complexity, channel estimation is not feasible in resource-constrained IoT devices. Instead, an adaptive random beamforming algorithm is proposed based on the Monte Carlo method, which provides high received power efficiency to multiple batteryless IoT devices without requiring complex channel estimation. The algorithm adapts the beamforming scheme based on partial feedback information, such as the received signal strength (RSS) value [140].

Recently, Intelligent Reflecting Surfaces (IRS) have gained significant attention for enhancing the performance of wireless-powered communications. Joint optimization in IRS-assisted wireless-powered communication networks (WPCNs) [141], [142], [143] and IRS-aided simultaneous wireless information and power transfer (SWIPT) [144] have been extensively studied. To overcome the double fading issue of conventional passive IRS, an active IRS-aided powered communication system is proposed, as illustrated in Fig. 25. Joint beamforming and resource allocation optimization are investigated for active IRS-aided WPCNs, where devices first harvest energy and then transmit information to a hybrid access point [145].

By utilizing advanced adaptive beamforming algorithms, the beams generated by phased arrays or active Intelligent Reflecting Surfaces (IRS) can be employed to select, track, and wirelessly power receivers, particularly in the case of moving objects or multiple nodes in a wireless communication network. Comprehensive consideration of the MWPT system, including channel state information (CSI), transmitter and receiver allocations, is crucial. The combination of advanced beam synthesis techniques and beamforming algorithms for energy transmission holds the potential for fast target tracking, optimal power transmission, and efficient resource allocation. However, it also poses challenges that need to be addressed.

IV. DISCUSSIONS

A. PERFORMANCE METRICS

Having discussed the techniques utilized to synthesize MWPT beams, the key parameters to compare when evaluating these techniques are:

a) *Transmission distance:* The transmission distance is proportional to the aperture size. For large transmission

distance, electrically-large antenna aperture is required. Especially for the near-field beam synthesis, e.g., the whisper antenna, nondiffractive antenna and focusing antenna, the transmission distance is comparable to the antenna aperture, and the transmission distance is limited by the aperture size.

b) *Antenna efficiency:* Resorting to these advanced beam synthesis techniques, the feeding network is complicated for the accurate phase and amplitude excitation to achieve special aperture filed distribution. Due to the complicated feeding network, the antenna radiation efficiency is always not high.

c) *Performance stability:* Overall, the performance stability of traditional antennas outperforms the reviewed advanced antennas, such as the whisper antennas and supergain antennas. This is due to the high sensitivity to phase and amplitude excitation changes. Particularly, the precise phase and amplitude excitation are required for supergain antennas, and a little excitation deviation would deteriorate the antenna performance, including gain and return loss.

d) *Beam manipulation:* Besides the electrical reconfigurable method, the beam can be steered through mechanical method. By changing the antenna physical or electric control configuration i.e., size, shape and feeding, the beam can be manipulation. Unlike traditional antennas, these advanced antennas perform well only when the special aperture field distribution is generated at the desired frequency, where the antenna implementation of physical dimension and feeding modes has certain constraints. Thus, these peculiarly synthesized beam manipulation is not easy. Furthermore, the existing overly complicated antenna feed network may become even more complex and costly.

e) *Fabrication:* Apart from supergain antenna, these antenna/antenna arrays mentioned above could be fabricated using traditional PCB technology. Unlike the conventional antenna, the supergain antenna could be fabricated by using refrigeration technology. For cooling, the whole system should be sealed to prevent the refrigerant leakage. Therefore, compared with other conventional antennas, the manufacturing process or packaging of the supergain antenna becomes more complicated.

f) *Safety:* Safety is an important issue for the human being as well as for the environment in high-power microwave power transmission. For the whisper beam and focused beam, the energy is converged only at the target location, and then the energy attenuates rapidly away from the target. Even at high power operation, both synthesized beams would have less effect on human activities and environment, while other synthesis beams are to be further investigated although the energy level at the target location is safe.

B. OUTSTANDING RESEARCH CHALLENGES

Although the remarkable progress on the research of the synthesized beam for transmitters is now being achieved, it is a pity that the MWPT system efficiency is still low which it hasn't been implemented in practice yet. To make it engineering, in addition to finding better beam synthesis technique for transmitters, we also need to address the following challenges:

a) *How to obtain the desired aperture distribution?* To realize high MWPT efficiency, the optimized aperture distribution is required. But these advanced synthesized beam technologies have only considered the free-space transmission efficiency or the RF-dc conversion efficiency of the receiver. For example, the current beam synthesis techniques, such as the whisper beam, supergain beam, focused beam and nondiffractive beam, were proposed to achieve efficient free-space transmission. However, the receivers with nonlinear rectifier diodes are not considered in the optimization of aperture field for the transmitters. For high RF-dc conversion efficiency of the rectenna, a flattop beam pattern launched by the transmitters was verified to ensure almost the same RF power output to each rectifying circuit element. However, the transmission efficiency between the transmitters and receivers is ignored. Thus, the system-level matching, CSI and allocations of the entire MWPT system should have been taken into account comprehensively, and the desired aperture distribution by joining advanced beamforming algorithm with beam synthesis will become an issue for high MWPT system efficiency.

b) *How to enhance the robustness?* To generate these advanced synthesized beams, precise phase and amplitude excitations are required. However, a small error of packaging and the manufacturing would greatly affect the excitations, and accordingly the performance of the transmitters deteriorates, such as the propagation property and operation frequency. Besides, these transmitters with abnormal beams have not been a thorough assessment for different environments at different RF power levels. Hence, problems associated with a robust estimation are to be resolved.

c) *How to implement engineering practices?* The transmitters with abnormal propagation property are feasible in theory, and these laboratory prototypes by using advanced beam synthesis technique are reasonable for research and proof of concept, but frequently encounters practical difficulties. For example, the industrial standard for mass-produced supergain antennas with film superconductor is yet to be developed. Besides, the perfect time reversal mirrors in free space are yet to be achieved for focused beam.

d) *How to reduce the overall size and complexity?* The transmission distance with finite aperture is limited, and a large-scale aperture antenna is required for long

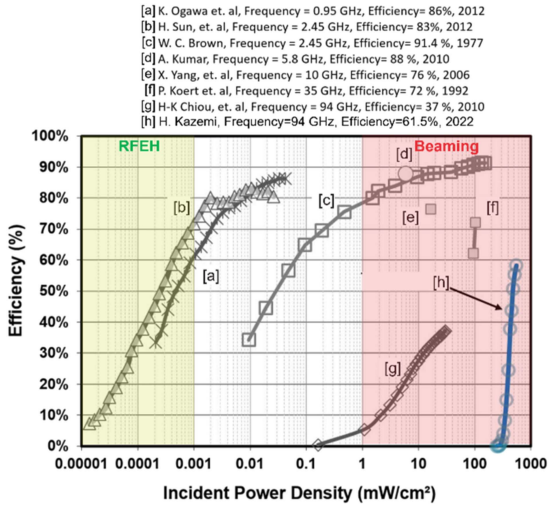

FIGURE 26. Conversion efficiency of several reported rectennas and rectifiers for different incident power densities.

transmission distance. Although the size of the super-gain antenna may be smaller than that of the antennas with other beam synthesis techniques, once the cooling systems, i.e., the stirling refrigerator, radome, vacuum pumping and stainless-steel cavity is included, the overall size of the antenna may become large. Besides, to achieve special aperture field distribution, a complicated feeding network should be designed for the accurate amplitude and phase of each element excitation. How to decrease the complexity and built a compact design for long transmission distance are to be addressed.

e) *How to realize integrated rectennas (MWPT receivers) based on advanced beams?* The key challenges outlined relate to the RF-RF efficiency of the antennas and the beamforming. For such high-power MWPT applications, additional challenges arise at the rectenna integration and RF-DC conversion stage. Fig. 26 summarizes the RF to DC efficiency of several reported rectennas for different incident power densities [139]. The desire to implement the reviewed beam synthesis techniques brings a semiconductor rectification challenge: high power handling, especially at mmWave and sub-THz frequencies [147], [148], calling for advanced compound semiconductors and novel device technologies for MWPT rectifiers at high-power levels.

C. SUMMARY

Advanced beam synthesis technologies are highly attractive and not only benefit MWPT but also have potential applications in telecommunications. Although some designs are already in a relatively close position to meet realistic engineering requirements, realizing long-distance MWPT at large power levels remains a long-term effort due to the inefficiency, size, and cost of existing MWPT implementations. These challenges can be further studied and developed in the future.

V. CONCLUSION

In this article, we present an overview of transmitting antennas employing advanced beam synthesis technologies, which are widely used in microwave wireless power transmission (MWPT) systems as discussed in the available literature. We explain the theory and concept of synthesized beams and showcase several antenna structures to analyze their critical features. The presented examples include advanced structures such as metamaterial-based, graphene-based, and superconductor-based antennas. We compare these antennas based on physical size, antenna efficiency, design complexity, and beam steerability for different application scenarios.

Through our analysis, it becomes evident that transmitting antennas for MWPT using advanced beam synthesis technologies currently face challenges such as high cost and large size. Most of the highly efficient MWPT systems employing advanced beam synthesis and beamforming algorithms are still in the theoretical stage, with few practical products available. The future research in achieving high-efficiency long-distance MWPT at large power levels is therefore a substantial task. In Section IV, we outline key challenges and research directions for enhancing the practicality of antennas in MWPT systems.

This review provides a comprehensive overview of beam synthesis techniques to guide antenna design. It introduces a wide range of design possibilities that enhance antenna performance. It is important to note that these advanced beam synthesis technologies are not limited to antenna structure design for MWPT systems. They can also be applied to beyond-5 G high-speed communication devices and high-resolution sensors in healthcare and industrial applications.

REFERENCES

[1] S. Sasaki, K. Tanaka, and K.-I. Maki, "Microwave power transmission technologies for solar power satellites," *Proc. IEEE*, vol. 101, no. 6, pp. 1438–1447, Jun. 2013.
[2] S. Yoshida, N. Hasegawa, and S. Kawasaki, "Experimental demonstration of microwave power transmission and wireless communication within a prototype reusable spacecraft," *IEEE Microw. Wireless Compon. Lett.*, vol. 25, no. 8, pp. 556–558, Aug. 2015.
[3] Y. Li et al., "GaN Schottky barrier diode-based wideband and medium-power microwave rectifier for wireless power transmission," *IEEE Trans. Electron Devices*, vol. 67, no. 10, pp. 4123–4129, Oct. 2020.
[4] X. Zhu, K. Jin, and Q. Hui, "Near-field power-focused directional radiation in microwave wireless power transfer system," *IEEE J. Emerg. Sel. Topics Power Electron.*, vol. 9, no. 1, pp. 1147–1156, Feb. 2021.
[5] P. E. Glaser, "Power from the sun: Its future," *Science*, vol. 162, no. 3856, pp. 857–861, 1968.
[6] N. Tesla, "Experiments with alternate currents of high potential and high frequency," *J. Inst. Elect. Eng.*, New York (State): W. J. Johnston, vol. 21, no. 97, pp. 39–58, 2010.
[7] W. C. Brown, "Experimental airborne microwave supported platform," Raytheon co burlington ma spencer lab, Final rept. Jun. 1964-Apr. 1965, Dec. 1965. [Online Available: https://apps.dtic.mil/sti/citations/AD0474925
[8] N. Tesla, "The transmission of electrical energy without wires as a means for furthering peace," *Elect. World Eng.*, vol. 1, pp. 21–24, 1905.
[9] R. Dickinson, "Reception-conversion subsystem (RXCV) transmission system," Raytheon Final Rep. Microwave Power, ER75-4386, 1975.
[10] R. Akiba et al., "ISY-METS rocket experiment," *Inst. Space Astronaut. Sci. Rep.*, vol. 652, pp. 1–13, 1993.

[11] [Online]. Available: https://www.kenkai.jaxa.jp/research/ssps/150301.html

[12] C. T. Rodenbeck et al., "Terrestrial microwave power beaming," *IEEE J. Microw.*, vol. 2, no. 1, pp. 28–43, Jan. 2022.

[13] C. T. Rodenbeck et al., "Microwave and millimeter wave power beaming," *IEEE J. Microw.*, vol. 1, no. 1, pp. 229–259, Jan. 2021.

[14] S. Naoyoshi et al., "Point-to-point microwave power transmission experiment," *Elect. Eng. Jpn.*, vol. 120, no. 1, pp. 33–39, 1997.

[15] G. Goubau and F. Schweering, "Free space beam transmission," *Microw. Power Eng.*, pp. 241–255, 1968. [Online]. Available: https://www.sciencedirect.com/science/article/abs/pii/B9781483197364500253

[16] M. Song et al., "Wireless power transfer based on novel physical concepts," *Nature Electron.*, vol. 4, pp. 707–716, 2021.

[17] X. Gu, S. Hemour, and K. Wu, "Far-field wireless power harvesting: Nonlinear modeling, rectenna design, and emerging applications," *Proc. IEEE*, vol. 110, no. 1, pp. 56–73, Jan. 2022.

[18] C. R. Valenta and G. D. Durgin, "Harvesting wireless power: Survey of energy-harvester conversion efficiency in far-field, wireless power transfer systems," *IEEE Microw. Mag.*, vol. 15, no. 4, pp. 108–120, Jun. 2014.

[19] N. Shinohara, "History and innovation of wireless power transfer via microwaves," *IEEE J. Microw.*, vol. 1, no. 1, pp. 218–228, Jan. 2021.

[20] A. Costanzo, F. Benassi, and G. Monti, "Wearable, energy-autonomous RF microwave systems: Chipless and energy-harvesting-based wireless systems for low-power, low-cost localization and sensing," *IEEE Microw. Mag.*, vol. 23, no. 3, pp. 24–38, Mar. 2022.

[21] M. Wagih et al., "Microwave-enabled wearables: Underpinning technologies, integration platforms, and next-generation roadmap," *IEEE J. Microw.*, vol. 3, no. 1, pp. 193–226, Jan. 2023.

[22] C. Song et al., "Advances in wirelessly powered backscatter communications: From antenna/RF circuitry design to printed flexible electronics," *Proc. IEEE*, vol. 110, no. 1, pp. 171–192, Jan. 2022.

[23] A. A. Eteng, H. H. Goh, S. K. A. Rahim, and A. Alomainy, "A review of metasurfaces for microwave energy transmission and harvesting in wireless powered networks," *IEEE Access*, vol. 9, pp. 27518–27539, 2021.

[24] J. Zhou, P. Zhang, J. Han, L. Li, and Y. Huang, "Metamaterials and metasurfaces for wireless power transfer and energy harvesting," *Proc. IEEE*, vol. 110, no. 1, pp. 31–55, Jan. 2022.

[25] E. Kwiatkowski, J. A. Estrada, A. López-Yela, and Z. Popović, "Broadband RF energy-harvesting arrays," *Proc. IEEE*, vol. 110, no. 1, pp. 74–88, Jan. 2022.

[26] M. Alibakhshikenari et al., "A comprehensive survey of 'metamaterial transmission-line based antennas: Design, challenges, and applications," *IEEE Access*, vol. 8, pp. 144778–144808, 2020.

[27] F. Zhao, D. Inserra, G. Wen, J. Li, and Y. Huang, "A high-efficiency inverse class-F microwave rectifier for wireless power transmission," *IEEE Microw. Wireless Compon. Lett.*, vol. 29, no. 11, pp. 725–728, Nov. 2019.

[28] S. Zhang, Y. Zeng, L. Song, S. Lou, and W. Wang, "A simplified model for calculating efficiency loss of aperture illumination with phase errors for microwave power transmission," *IEEE Antennas Wireless Propag. Lett.*, vol. 20, no. 4, pp. 468–472, Apr. 2021.

[29] M. Alibakhshikenari, B. Virdee, and L. Azpilicueta, "Optimum power transfer in RF front end systems using adaptive impedance matching technique," *Sci. Rep.*, vol. 11, 2021, Art. no. 11825.

[30] M. Alibakhshikenari, B. S. Virdee, C. H. See, R. A. Abd-Alhameed, F. Falcone, and E. Limiti, "Automated reconfigurable antenna impedance for optimum power transfer," in *Proc. IEEE Asia-Pacific Microw. Conf.*, 2019, pp. 1461–1463.

[31] L. Wang, W. Dou, and H. Meng, "Study of millimeter wave spatial beam synthesis based on quasi-optical technology," in *Proc. IEEE 5th Asia-Pacific Conf. Antennas Propag.*, 2016, pp. 333–334.

[32] Z. Zhao, X. Ding, K. Zhang, J. Fu, and Q. Wu, "2-D airy beam generation and manipulation utilizing metasurface," *IEEE Trans. Magn.*, vol. 58, no. 2, Feb. 2022, Art. no. 2500605.

[33] Y. T. Chen, X. Q. Lin, Y. Fan, and S. L. Liu, "Generation of Ka-band accelerating and self-bending beam by series-fed patch array," *IEEE Antennas Wireless Propag. Lett.*, vol. 20, no. 2, pp. 239–243, Feb. 2021.

[34] J. Greason, "Non-Gaussian beams for long-distance wireless power transmission," U.S. Patent US20200195057A1, Jun. 18, 2020.

[35] P. Lu, K. Huang, Y. Yang, B. Zhang, F. Cheng, and C. Song, "Space matching for highly efficient microwave wireless power transmission system: Theory, prototype, and experiments," *IEEE Trans. Microw. Theory Techn.*, vol. 69, no. 3, pp. 1985–1998, Mar. 2021.

[36] B. P. Kumar and G. R. Branner, "Array current distributions to generate flat-topped beams," in *Proc. Antennas Propag. Soc. Int. Symp.*, 1995, pp. 1810–1813.

[37] N. Takabayashi, N. Shinohara, T. Mitani, M. Furukawa, and T. Fujiwara, "Rectification improvement with flat-topped beams on 2.45-GHz rectenna arrays," *IEEE Trans. Microw. Theory Techn.*, vol. 68, no. 3, pp. 1151–1163, Mar. 2020.

[38] N. Takabayashi, N. Shinohara, and T. Fujiwara, "Array pattern synthesis of flat-topped beam for microwave power transfer system at volcanoes," in *Proc. IEEE Wireless Power Transfer Conf.*, 2018, pp. 1–4.

[39] N. T. Nguyen, R. Sauleau, and L. Le Coq, "Reduced-size double-shell lens antenna with flat-top radiation pattern for indoor communications at millimeter waves," *IEEE Trans. Antennas Propag.*, vol. 59, no. 6, pp. 2424–2429, Jun. 2011.

[40] L. Wu, A. Zielinski, J. S. Bird, and R. Kieser, "Synthesis of symmetric flattop radiation patterns," *IEEE J. Ocean. Eng.*, vol. 21, no. 1, pp. 105–108, Jan. 1996.

[41] J. Zhou, H. Huang, H. Sun, and Z. Liu, "Design and realization of a flat-top shaped-beam antenna array," *Prog. Electromagn. Res. Lett*, vol. 5, pp. 159–166, 2008.

[42] Z. Zhang, N. Liu, S. Zuo, Y. Li, and G. Fu, "Wideband circularly polarized array antenna with flat-top beam pattern," *Inst. Eng. Technol. Microw. Antennas Propag.*, vol. 9, no. 8, pp. 755–761, 2015.

[43] X. Cai, W. Ge, and Y. Guo, "A compact rectenna with flattop angular coverage for RF energy harvesting," *IEEE Antennas Wireless Propag. Lett.*, vol. 20, no. 7, pp. 1307–1311, Jul. 2021.

[44] A. K. Singh, M. P. Abegaonkar, and S. K. Koul, "Wide angle beam steerable high gain flat top beam antenna using graded index metasurface lens," *IEEE Trans. Antennas Propag.*, vol. 67, no. 10, pp. 6334–6343, Oct. 2019.

[45] M. Monavar, S. Shamsinejad, R. Mirzavand, J. Melzer, and P. Mousavi, "Beam-steering SIW leaky-wave subarray with flat-topped footprint for 5G applications," *IEEE Trans. Antennas Propag.*, vol. 65, no. 3, pp. 1108–1120, Mar. 2017.

[46] N. Takabayashi, K. Kawai, M. Mase, N. Shinohara, and T. Mitani, "Large-scale sequentially-fed array antenna radiating flat-top beam for microwave power transmission to drones," *IEEE J. Microw.*, vol. 2, no. 2, pp. 297–306, Apr. 2022.

[47] G. S. Lipworth et al., "A large planar holographic reflectarray for Fresnel-zone microwave wireless power transfer at 5.8 GHz," in *Proc. IEEE Microw. Theory Techn. Soc. Int. Microw. Symp.*, 2018, pp. 964–967.

[48] Z. Bouchal, "Nondiffracting optical beams: Physical properties, experiments and applications," *Czechoslovak J. Phys.*, vol. 53, no. 7, pp. 537–578, 2003.

[49] J. Durnin, "Exact solutions for nondiffracting beams I: The scalar theory," *J. Opt. Soc. Amer.*, vol. 4, no. 4, pp. 651–654, 1987.

[50] L. Auger, S. Abielmona, and C. Caloz, "Generation of Bessel beams by two-dimensional antenna arrays using sub-sampled distributions," *IEEE Trans. Antennas Propag.*, vol. 61, no. 4, pp. 1838–1849, Apr. 2013.

[51] J. Durnin, J. Miceli, and H. Eberly, "Diffraction-free beam," *Phys. Rev. Lett.*, vol. 58, pp. 1499–1501, 1987.

[52] A. Vasara, J. Turunen, and T. Friberg, "Realization of general nondiffracting beams with computer-generated holograms," *J. Opt. Soc. Amer.*, vol. 6, no. 11, pp. 1748–1754, 1989.

[53] J. Cox and C. Dibble, "Nondiffracting beam from a spatially filtered Fabry-Perot resonator," *J. Opt. Soc. Amer.*, vol. 9, pp. 282–286, 1992.

[54] G. Scott and N. Mcardle, "Efficient generation of nearly diffraction-free beams using an axicon," *Proc. SPIE*, vol. 31, no. 12, pp. 2640–2643.

[55] M. Herman and A. Wiggins, "High efficiency diffractionless beams of constant size and intensity," *Appl. Opt.*, vol. 33, no. 31, pp. 7297–7306.

[56] C. Pfeiffer and A. Grbic, "Controlling vector Bessel beams with metasurfaces," *Phys. Rev. Appl.*, vol. 2, no. 4, 2014, Art. no. 044012.

[57] Z. Wang et al., "High-efficiency generation of Bessel beams with transmissive metasurfaces," *Appl. Phys. Lett.*, vol. 112, no. 19, 2018, Art. no. 191901.

[58] M. R. Akram et al., "Highly efficient generation of Bessel beams with polarization insensitive metasurfaces," *Opt. Exp.*, vol. 27, no. 7, pp. 9467–9480, 2019.

[59] W. T. Chen et al., "Generation of wavelength-independent subwavelength Bessel beams using metasurfaces," *Light: Sci. Appl.*, vol. 6, no. 5, 2017, Art. no. e16259.

[60] M. Q. Qi, W. X. Tang, and T. J. Cui, "A broadband Bessel beam launcher using metamaterial lens," *Sci. Rep.*, vol. 5, no. 1, pp. 1–11, 2015.

[61] Y. B. Li, B. G. Cai, X. Wan, and T. J. Cui, "Diffraction-free surface waves by metasurfaces," *Opt. Lett.*, vol. 39, no. 20, pp. 5888–5891, 2014.

[62] Y. C. Zhong and Y. J. Cheng, "Ka-band wideband large depth-of-field beam generation through a phase shifting surface antenna," *IEEE Trans. Antenn. Propag.*, vol. 64, no. 12, pp. 5038–5045, Dec. 2016.

[63] B. Cheng et al., "Frequency scanning non-diffractive beam by metasurface," *Appl. Phys. Lett.*, vol. 110, no. 3, 2017, Art. no. 031108.

[64] A. Mazzinghi et al., "Large depth of field pseudo-Bessel beam generation with a RLSA antenna," *IEEE Trans. Antennas Propag.*, vol. 62, no. 8, pp. 3911–3919, Aug. 2014.

[65] M. Ettorre, S. C. Pavone, M. Casaletti, and M. Albani, "Experimental validation of Bessel beam generation using an inward Hankel aperture distribution," *IEEE Trans. Antennas Propag.*, vol. 63, no. 6, pp. 2539–2544, Jun. 2015.

[66] S. C. Pavone, M. Ettorre, and M. Albani, "Analysis and design of Bessel beam launchers: Longitudinal polarization," *IEEE Trans. Antennas Propag.*, vol. 64, no. 6, pp. 2311–2318, Jun. 2016.

[67] M. Ettorre and A. Grbic, "Generation of propagating Bessel beams using leaky-wave modes," *IEEE Trans. Antennas Propag.*, vol. 60, no. 8, pp. 3605–3613, Aug. 2012.

[68] M. A. Salem, A. H. Kamel, and E. Niver, "Microwave Bessel beams generation using guided modes," *IEEE Trans. Antennas Propag.*, vol. 59, no. 6, pp. 2241–2247, Jun. 2011.

[69] M. Ettorre, S. M. Rudolph, and A. Grbic, "Generation of propagating Bessel beams using leaky-wave modes: Experimental validation," *IEEE Trans. Antennas Propag.*, vol. 60, no. 6, pp. 2645–2653, Jun. 2012.

[70] P. Lu et al., "Design of TE-polarized Bessel antenna in microwave range using leaky-wave modes," *IEEE Trans. Antenna Propag.*, vol. 66, no. 1, pp. 32–41, Jan. 2018.

[71] P. Lu, F. Cheng, Y. Yang, B. Zhang, and K. M. Huang, "A reconfigurable Bessel antenna for near-field beam deflection," *Microw. Opt. Technol. Lett.*, vol. 62, no. 5, pp. 2104–2108, 2020.

[72] Y. F. Wu and Y. J. Cheng, "Proactive conformal antenna array for near-field beam focusing and steering based on curved substrate integrated waveguide," *IEEE Trans. Antenna Propag.*, vol. 67, no. 4, pp. 2354–2363, Apr. 2019.

[73] S. Liu et al., "Anomalous refraction and nondiffractive Bessel-beam generation of terahertz waves through transmission-type coding metasurfaces," *Amer. Chem. Soc. Photon.*, vol. 3, no. 10, pp. 1968–1977, 2016.

[74] Y. C. Zhong and Y. J. Cheng, "Wideband quasi-nondiffraction beam with accurately controllable propagating angle and depth-of-field," *IEEE Trans. Antenna Propag.*, vol. 65, no. 10, pp. 5035–5042, Oct. 2017.

[75] Y. C. Zhong and Y. J. Cheng, "Generating and steering quasi-nondiffractive beam by near-field planar Risley prisms," *IEEE Trans. Antenna Propag.*, vol. 68, no. 12, pp. 7767–7776, Dec. 2020.

[76] Q. Liu, P. Lu, K. M. Huang, and D. Z. Qian, "Non-diffraction surface wave with controllable deflection angle by using metasurfaces," *J. Appl. Phys.*, vol. 128, no. 19, 2020, Art. no. 195104.

[77] T. Zeng et al., "Generation of nondiffraction beams by using graphene based metasurface in terahertz regime," *Microw. Opt. Techn. Lett.*, vol. 63, no. 4, pp. 1126–1133, 2021.

[78] L. J. Chu, "Physical limitations of omnidirectional antennas," *J. Appl. Phys.*, vol. 19, pp. 1163–1175, 1948.

[79] A. I. Uzkov, "An approach to the problem of optimum directive antennae design," *Comptes Rendus (Doklady) l' Acad. des Sci. l' URSS*, vol. 53, pp. 35–38, 1946.

[80] J. M. Lugo, J. Almeida Goes de, A. Louzir, P. Minard, D. Lo Hine Tong, and C. Person, "Design, optimization and characterization of a superdirective antenna array," in *Proc. 7th Eur. Conf. Antennas Propag.*, 2013, pp. 3736–3739.

[81] S. M. Mazinani and H. R. Hassani, "Superdirective wideband array of planar monopole antenna with loading plates," *IEEE Antennas Wireless Propag. Lett.*, vol. 9, pp. 978–981, 2010.

[82] A. Haskou, A. Sharaiha, and S. Collardey, "Design of small parasitic loaded superdirective end-fire antenna arrays," *IEEE Trans. Antennas Propag.*, vol. 63, no. 12, pp. 5456–5464, Dec. 2015.

[83] A. Clemente, C. Jouanlanne, and C. Delaveaud, "Analysis and design of a four-element superdirective compact dipole antenna array," in *Proc. 11th Eur. Conf. Antennas Propag.*, 2017, pp. 2700–2704.

[84] O. S. Kim, S. Pivnenko, and O. Breinbjerg, "Superdirective magnetic dipole array as a first-order probe for spherical near-field antenna measurements," *IEEE Trans. Antennas Propag.*, vol. 60, no. 10, pp. 4670–4676, Oct. 2012.

[85] S. Dakhli, H. Rmili, J. Floc'h, and F. Choubani, "A novel compact and superdirective two elements antenna array," in *Proc. Loughborough Antennas Propag. Conf.*, 2016, pp. 1–5.

[86] B. Sentucq, A. Sharaiha, and S. Collardey, "Superdirective metamaterial-inspired electrically small antenna arrays," in *Proc. 7th Eur. Conf. Antennas Propag.*, 2013, pp. 151–155.

[87] A. Haskou, S. Collardey, and A. Sharaiha, "Small array design using parasitic superdirective antennas," in *Proc. 10th Eur. Conf. Antennas Propag.*, 2016, pp. 1–4.

[88] A. Haskou, S. Collardey, and A. Sharaiha, "A design methodology for impedance-matched electrically small parasitic superdirective arrays," in *Proc. IEEE Int. Symp. Antennas Propag. United Nations Secur. Council/Int. Union Radio Sci. Nat. Radio Sci. Meeting*, 2015, pp. 1852–1853.

[89] B. Sentucq, A. Sharaiha, and S. Collardey, "Superdirective compact parasitic array of metamaterial-inspired electrically small antenna," in *Proc. Int. Workshop Antenna Technol.*, 2013, pp. 269–272.

[90] T. Kokkinos and A. P. Feresidis, "Electrically small superdirective endfire arrays of metamaterial-inspired low-profile monopoles," *IEEE Antennas Wireless Propag. Lett.*, vol. 11, pp. 568–571, 2012.

[91] T. I. Lee and Y. E. Wang, "A mode-based supergain approach with closely coupled monopole pair," in *Proc. IEEE Int. Symp. Antennas Propag. Soc.*, 2007, pp. 5901–5904.

[92] Z. Chen and Z. Shen, "A conformal cavity-backed supergain slot antenna," in *Proc. IEEE Int. Symp. Antennas Propag. Soc.*, 2014, pp. 1288–1289.

[93] L. P. Ivrissimtzis, M. J. Lancaster, and N. M. Alford, "A high gain YBCO antenna array with integrated feed and balun," *IEEE Trans. Appl. Supercond.*, vol. 5, no. 2, pp. 3199–3202, Jun. 1995.

[94] L. P. Ivrissimtzis, M. J. Lancaster, and N. M. Alford, "Supergain printed arrays of closely spaced dipoles made of thick film high-Tc superconductors," *IEE Proc. Microw. Antennas Propag.*, vol. 142, no. 1, pp. 26–34, 1995.

[95] A. Buffi, P. Nepa, and G. Manara, "Design criteria for near-field-focused planar arrays," *IEEE Antennas Propag. Mag.*, vol. 54, no. 1, pp. 40–50, Feb. 2012.

[96] M. Bogosanovic, A. Al Anbury, and G. Emms, "Metal plate lens in a focused beam system for microwave material testing," in *Proc. Microw. Conf.*, 2008, pp. 1–4.

[97] A. Grbic and R. Merlin, "Near-field focusing plates and their design," *IEEE Trans. Antennas Propag.*, vol. 56, no. 10, pp. 3159–3165, Oct. 2008.

[98] P. Piksa and P. Cerny, "Near field measurement of Gaussian beam behind dielectric lens," in *Proc. 17th Int. Conf. Radioelektronika*, 2007, pp. 1–4.

[99] M. Moresco and E. Zilli, "Focused aperture microwave antennas operating in the near-field zone," *Int. J. Infrared Millimeter Waves*, vol. 3, pp. 279–293, 1982.

[100] E. Ongareau, E. Marouby, and J. Levrel, "Charts for a quick design of spot-focusing corrugated horn lens antennas," in *Proc. Int. Symp. Antennas Propag. Soc.*, 1994, vol. 2, pp. 986–989.

[101] A. Dhouibi, S. N. Burokur, A. de Lustrac, and A. Priou, "Compact metamaterial-based substrate-integrated Luneburg lens antenna," *IEEE Antennas Wireless Propag. Lett.*, vol. 11, pp. 1504–1507, 2012.

[102] A. Pereira and N. Carvalho, "Quasioptics for increasing the beam efficiency of wireless power transfer systems," *Sci. Rep.*, vol. 12, 2022, Art. no. 20894.

[103] J. Huang, "Microstrip reflectarray," in *Proc. Antennas Propag. Soc. Int. Symp. Dig.*, 1991, vol. 2, pp. 612–615.

[104] S. X. Yu and L. Li, "Design of near-field focused power-combining reflectarray," in *Proc. 10th Eur. Conf. Antennas Propag.*, 2016, pp. 1–2.

[105] T. T. Chia, T. K. Chua, and Z. N. Chen, "Design of a C-band reflectarray antenna for near-field applications," in *Proc. Int. Conf. Electromagn. Adv. Appl.*, 2019, pp. 1028–1031.

[106] H. T. Chou, Y.-X. Liu, X.-Y. Dong, and B.-Q. You, "Reflectarray antennas for near-field focused radiation: Numerical modeling, synthesis and realistic realization," in *Proc. IEEE Int. Conf. Wireless Inf. Technol. Syst.*, 2012, pp. 1–4.

[107] M. M. Tahseen and A. A. Kishk, "Flexible and portable textile-reflectarray backed by frequency selective surface," *IEEE Antennas Wireless Propag. Lett.*, vol. 17, no. 1, pp. 46–49, Jan. 2018.

[108] H. T. Chou, L. R. Kuo, K. L. Hung, H. H. Chou, and S. C. Tuan, "Analysis of elliptic reflector antennas in near field focused RFID applications," in *Proc. IEEE Antennas Propag Soc. Int. Symp.*, 2009, pp. 1–4.

[109] S. Xiao, S. Altunc, P. Kumar, E. C. Baum, and K. H. Schoenbach, "A reflector antenna for focusing subnanosecond pulses in the near field," *IEEE Antennas Wireless Propag. Lett.*, vol. 9, pp. 12–15, 2010.

[110] H.-T. Chou, H.-T. Cheng, S.-J. Chou, L.-R. Kuo, A. Buffi, and P. Nepa, "Dome-shaped ellipsoidal reflector antenna for UHF-RFID readers with confined near-field detection region," *IEEE Antennas Wireless Propag. Lett.*, vol. 16, pp. 2505–2508, 2017.

[111] H.-T. Chou and P. Nepa, "Multi-facet focused microwave antennas," in *Proc. IEEE-Amer. Phys. Soc. Topical Conf. Antennas Propag. Wireless Commun.*, 2016, pp. 294–297.

[112] H. Chou and P. Nepa, "Near-field focused radiation by two edgecoupled microstrip antenna arrays," in *Proc. Int. Union Radio Sci. Int. Symp. Electromagn. Theory*, 2016, pp. 709–712.

[113] H. T. Chou, K. L. Hung, and H. H. Chou, "Design of periodic antenna arrays with the excitation phases synthesized for optimum near-field patterns via steepest descent method," *IEEE Trans. Antennas Propag.*, vol. 59, no. 11, pp. 4342–4345, Nov. 2011.

[114] J. Alvarez, R. G. Ayestaran, G. Leon, J. A. Lopez-Fernandez, L. F. Herran, and F. Las-Heras, "Optimization framework on antenna arrays for near field multifocusing," in *Proc. IEEE Int. Symp. Antennas Propag.*, 2012, pp. 1–2.

[115] Y. F. Wu, Y. J. Cheng, and Y. Fan, "3D beamforming method for near-field-focused active phased array: 3D scanning and 3D polarization manipulating," in *Proc. Int. Appl. Comput. Electromagn. Soc. China Symp.*, 2021, pp. 1–2.

[116] Z. X. Huang and Y. J. Cheng, "Synthesis of sparse near-field focusing antenna arrays based on Bayesian compressive sensing," in *Proc. IEEE Int. Conf. Comput. Electromagn.*, 2018, pp. 1–4.

[117] R. G. Ayestarán, M. R. Pino, and P. Nepa, "Synthesis of near field focused arrays including far field constrains," in *Proc. Int. Appl. Comput. Electromagn. Soc. Symp.-Italy*, 2017, pp. 1–2.

[118] J. Alvarez, R. G. Ayestaran, G. Leon, L. F. Herran, J. A. Lopez, and F. Las-Heras, "Near field multifocusing on antenna arrays via nonconvex optimization," *Int. Eng. Technol. Microw., Antennas Propag.*, vol. 8, no. 10, pp. 754–764, 2014.

[119] X. Wang, S. Sha, J. He, L. Guo, and M. Lu, "Wireless power delivery to low-power mobile devices based on retro-reflective beamforming," *IEEE Antennas Wireless Propag. Lett.*, vol. 13, pp. 919–922, 2014.

[120] H. Koo et al., "Retroreflective transceiver array using a novel calibration method based on optimum phase searching," *IEEE Trans. Ind. Electron.*, vol. 68, no. 3, pp. 2510–2520, Mar. 2021.

[121] P. D. Hilario, S. K. Podilchak, S. Rotenber, G. Goussetis, and J. Lee, "Circularly polarized retrodirective antenna array for wireless power transmission," *IEEE Trans. Antennas Propag.*, vol. 68, no. 4, pp. 2743–2752, Apr. 2020.

[122] R. Ibrahim et al., "Experiments of time-reversed pulse waves for wireless power transmission in an indoor environment," *IEEE Trans. Microw. Theory Techn.*, vol. 64, no. 7, pp. 2159–2170, Jun. 2016.

[123] C. Oestges, A. D. Kim, G. Papanicolaou, and A. J. Paulraj, "Characterization of space-time focusing in time-reversed random fields," *IEEE Trans. Antennas Propag.*, vol. 53, no. 1, pp. 283–293, Jan. 2005.

[124] D. Belo, D. C. Ribeiro, P. Pinho, and N. B. Carvalho, "A selective, tracking, and power adaptive far-field wireless power transfer system," *IEEE Trans. Microw. Theory Techn.*, vol. 67, no. 9, pp. 3856–3866, Sep. 2019.

[125] D. Belo and N. B. Carvalho, "An OOK chirp spread spectrum backscatter communication system for wireless power transfer applications," *IEEE Trans. Microw. Theory Techn.*, vol. 69, no. 3, pp. 1838–1845, Mar. 2021.

[126] D. Cassereau and M. Fink, "Time-reversal of ultrasonic fields III. Theory of the closed time-reversal cavity," *IEEE Trans. Ultrason., Ferroelect., Freq. Control*, vol. 39, no. 5, pp. 579–592, Sep. 1992.

[127] M. Fink, "Time reversed acoustics," *Phys. Today*, vol. 50, no. 3, pp. 34–40, 1997.

[128] G. Lerosey, J. Rosny de, A. Tourin, A. Derode, G. Montaldo, and M. Fink, "Time reversal of electromagnetic waves," *Phys. Rev. Lett.*, vol. 92, no. 19, 2004, Art. no. 193904.

[129] M. Frazier, B. Taddese, T. Antonsen, and S. M. Anlage, "Nonlinear time reversal in a wave chaotic system," *Phys. Rev. Lett.*, vol. 110, no. 6, 2013, Art. no. 063902.

[130] M. Frazier, B. Taddese, B. Xiao, T. Antonsen, E. Ott, and S. M. Anlage, "Nonlinear time reversal of classical waves: Experiment and model," *Phys. Rev. E*, vol. 88, no. 6, 2013, Art. no. 062910.

[131] Y. Chen et al., "Time-reversal wireless paradigm for green Internet of Things: An overview," *IEEE Internet Things J.*, vol. 1, no. 1, pp. 81–98, Feb. 2014.

[132] F. Cangialosi, T. Grover, P. Healey, T. Furman, A. Simon, and S. M. Anlage, "Time reversed electromagnetic wave propagation as a novel method of wireless power transfer," in *Proc. IEEE Wireless Power Transfer Conf.*, 2016, pp. 1–4.

[133] D. Zhao and M. Zhu, "Generating microwave spatial fields with arbitrary patterns," *IEEE Antennas Wireless Propag. Lett.*, vol. 15, pp. 1739–1742, 2016.

[134] M.-L. Ku, Y. Han, H.-Q. Lai, Y. Chen, and K. J. R. Liu, "Power waveforming: Wireless power transfer beyond time reversal," *IEEE Trans. Signal Process.*, vol. 64, no. 22, pp. 5819–5834, Nov. 2016.

[135] B. Li, S. Liu, H.-L. Zhang, B.-J. Hu, D. Zhao, and Y. Huang, "Wireless power transfer based on microwaves and time reversal for indoor environments," *IEEE Access*, vol. 7, pp. 114897–114908, 2019.

[136] H. S. Park and S. K. Hong, "Investigation of time-reversal based far-field wireless power transfer from antenna array in a complex environment," *IEEE Access*, vol. 8, pp. 66517–66528, 2020.

[137] Y. Zhang, Z. Shi, J. Wu, M. Tian, H. Zhang, and B. Zhao, "A fast-beamforming technique for blind-adaptive wireless power transfer towards free-flying insects," in *Proc. IEEE Biomed. Circuits Syst. Conf.*, 2019, pp. 1–4.

[138] M. R. V. Moghadam and R. Zhang, "Node placement and distributed magnetic beamforming optimization for wireless power transfer," *IEEE Trans. Signal Inf. Process. Over Netw.*, vol. 4, no. 2, pp. 264–279, Jun. 2018.

[139] X. Lan, Q. Chen, L. Cai, and L. Fan, "Buffer-aided adaptive wireless powered communication network with finite energy storage and data buffer," *IEEE Trans. Wireless Commun.*, vol. 18, no. 12, pp. 5764–5779, Dec. 2019.

[140] Y. Zhao, X. Li, C.-Z. Xu, and S. Zhang, "Adaptive random beamforming for MIMO wireless power transfer system," in *Proc. IEEE Wireless Commun. Netw. Conf.*, 2018, pp. 1–6.

[141] Y. Zheng, S. Bi, Y. J. Zhang, Z. Quan, and H. Wang, "Intelligent reflecting surface enhanced user cooperation in wireless powered communication networks," *IEEE Wireless Commun. Lett.*, vol. 9, no. 6, pp. 901–905, Jun. 2020.

[142] Q. Wu, X. Zhou, W. Chen, J. Li, and X. Zhang, "IRS-aided WPCNs: A new optimization framework for dynamic IRS beamforming," *IEEE Trans. Wireless Commun.*, vol. 21, no. 7, pp. 4725–4739, Jul. 2022.

[143] Y. Zou et al., "Wireless powered intelligent reflecting surfaces for enhancing wireless communications," *IEEE Trans. Veh. Technol.*, vol. 69, no. 10, pp. 12369–12373, Oct. 2020.

[144] C. Pan et al., "Intelligent reflecting surface aided MIMO broadcasting for simultaneous wireless information and power transfer," *IEEE J. Sel. Areas Commun.*, vol. 38, no. 8, pp. 1719–1734, Aug. 2020.

[145] P. Zeng, D. Qiao, Q. Wu, and Y. Wu, "Throughput maximization for active intelligent reflecting surface-aided wireless powered communications," *IEEE Wireless Commun. Lett.*, vol. 11, no. 5, pp. 992–996, May 2022.

[146] H. Kazemi, "61.5% efficiency and 3.6 kW/m^2 power handling rectenna circuit demonstration for radiative millimeter wave wireless power transmission," *IEEE Trans. Microw. Theory Techn.*, vol. 70, no. 1, pp. 650–658, Jan. 2022.

[147] M. Wagih, A. S. Weddell, and S. Beeby, "Millimeter-wave power harvesting: A review," *IEEE Open J. Antennas Propag.*, vol. 1, pp. 560–578, 2020.

[148] S. Mizojiri and K. Shimamura, "Recent progress of wireless power transfer via sub-THz wave," in *Proc. IEEE Asia-Pacific Microw. Conf.*, 2019, pp. 705–707.